

Paleoceanography and Paleoclimatology

RESEARCH ARTICLE

10.1029/2018PA003455

Key Points:

- The Western Pacific Warm Pool was warmer in the early Holocene and cooled toward the present because of changes in insolation-driven tropical Pacific mean state
- The Holocene cooling was mostly felt in the southern Indo-Pacific Warm Pool regions likely responding to a complex combination of climatic processes
- The deglacial Indo-Pacific Warm Pool temperatures raised gradually similar to the atmospheric CO₂ and/or Antarctica temperature changes

Supporting Information:

- Supporting Information S1
- Data Set S1

Correspondence to:

P. Moffa-Sanchez,
paola.l.moffa-sanchez@durham.ac.uk

Citation:





Moffa-Sanchez, P., Rosenthal, Y., Babila, T. L., Mohtadi, M., & Zhang, X. (2019). Temperature evolution of the Indo-Pacific Warm Pool over the Holocene and the last deglaciation. *Paleoceanography and Paleoclimatology*, 34. <https://doi.org/10.1029/2018PA003455>

Received 4 AUG 2018

Accepted 2 JUN 2019

Accepted article online 11 JUN 2019

Temperature Evolution of the Indo-Pacific Warm Pool Over the Holocene and the Last Deglaciation

Paola Moffa-Sanchez^{1,2} , Yair Rosenthal¹, Tali L. Babila³ , Mahyar Mohtadi⁴ , and Xu Zhang^{5,6} 

¹Department of Marine and Coastal Sciences, Rutgers University, New Brunswick, NJ, USA, ²Department of Geography, Durham University, Durham, UK, ³Ocean and Earth Science National Oceanography Centre, University of Southampton, Southampton, UK, ⁴MARUM – Center for Marine Environmental Sciences, University of Bremen, Bremen, Germany, ⁵Key Laboratory of Western China's Environmental Systems (Ministry of Education), College of Earth and Environmental Sciences, Lanzhou University, Lanzhou, China, ⁶Alfred Wegener Institute Helmholtz Centre for Polar and Marine Research, Bremerhaven, Germany

Abstract The Indo-Pacific Warm Pool (IPWP) contains the warmest surface ocean waters on our planet making it a major source of heat and moisture to the atmosphere. Changes in the extent and position of the IPWP likely impacted the tropical and global climate in the past and may also do in the future. With the aim to put recent ocean changes into a longer temporal context, we present new paleoceanographic sea surface temperature reconstructions from the heart of the Western Pacific Warm Pool, which is the warmest region within the IPWP, across the last 17,000 years. To provide an improved spatial and temporal regional context we use new and published sea surface temperature records from the IPWP and update previous compilation efforts (Linsley et al., 2010, <https://doi.org/10.1038/ngeo1920>). We similarly conclude that the IPWP was warmer in the early Holocene compared to the late Holocene. However, with the new data we are able to argue against a western displacement/expansion of the IPWP and suggest a warmer southern IPWP in the early Holocene. We explore the potential drivers of the Holocene IPWP cooling and propose a combination of processes including changes in the monsoonal winds associated with the position of the rain belt, the tropical Pacific mean climate, and upper water column mixing. The proposed climatic processes differentially impacted the IPWP subregions resulting in spatially diverse trends. Additionally, the late deglacial section of the records mostly show a gradual IPWP warming similar in structure to the atmospheric CO₂ and/or Antarctica rising temperatures.

1. Introduction

Studying the millennial climate trends of our current interglacial provides us with the necessary context to put recent climate into a longer perspective and offers a unique opportunity to test numerical models that are used for future climate projections. Yet, controversy remains on the global and regional temperature evolution of the Earth's climate over the Holocene (Lohmann et al., 2013; Marcott et al., 2013; Liu, Zhu, et al., 2014). Proxy temperature records, mostly composed of marine records and interpreted as representing mean annual temperature, reveal a global cooling from 5,500 to 100 years before present (BP) of ~0.7 °C, although regional compilations paint a more complex temperature evolution (Marcott et al., 2013). In contrast, climate models consistently simulate a mean annual temperature warming trend over the Holocene primarily caused by the small increase in atmospheric CO₂ and receding northern hemisphere ice sheets throughout the Holocene (Liu, Zhu, et al., 2014). This data-model discrepancy can be due to several shortcomings including seasonal biases embedded in the paleotemperature proxies and/or a weak climate model response to orbital forcing perhaps associated with albedo-related feedback parameterizations such as snow, ice, vegetation, high-latitude climate, and clouds (Liu, Zhu, et al., 2014; Timmermann et al., 2014; Marsicek et al., 2018). Improving the spatial coverage of surface temperature reconstructions will allow us to better deconvolve regional from global signals and elucidate the forcings and the climatic feedbacks that drive millennial-scale variability.

The focus of this study is the tropical western Pacific, an area that hosts the warmest temperatures in the world's oceans. The area with annual sea surface temperatures (SST) above 28 °C is typically referred to as the Western Pacific Warm Pool (WPWP; e.g., Wyrтки, 1989), which is the eastern and warmest sector of

the larger Indo-Pacific Warm Pool (IPWP; Figure 1). Since SST are higher than the estimated threshold for atmospheric deep convection (Fu et al., 1994), the IPWP is a major source of heat and moisture to the atmosphere and hence a location of deep atmospheric convection and heavy local rainfall. Small changes in the SST of the IPWP can therefore influence the location and strength of convection in the rising limb of the Hadley and Walker circulations, perturbing planetary-scale atmospheric circulation and tropical hydrology (Neale & Slingo, 2003; Wang & Mehta, 2008). These changes in the SST can also influence the uptake of heat and its storage in the thermocline depths as well as its ability to redistribute heat via net transport to the Indian Ocean through the Indonesian Throughflow (ITF; Gordon & Fine, 1996; Sprintall et al., 2014).

Collectively, these processes constitute important feedbacks, which highlight the climatic significance of the IPWP through its atmospheric teleconnections to the global climate system (e.g., Palmer & Mansfield, 1984; Trenberth et al., 1998). Recent observations show a freshening and expansion of the WPWP over the last ~50 years hypothesized to be a response of rising greenhouse gas concentrations (Cravatte et al., 2009; Durack et al., 2012; Weller et al., 2016). However, because of the short temporal coverage of instrumental records and conflicting model-data results (Liu, Zhu, et al., 2014), considerable uncertainty still remains about the longer variability of the IPWP and the accuracy of the current models in predicting the future response of tropical Pacific climate to rising greenhouse gases, specifically atmospheric CO₂ (IPCC, 2013). The location of the IPWP lies at a crossroads of different climatological processes, and hence, large uncertainty still exists on the mechanisms that govern spatial and temporal variabilities of the SST in the IPWP. Despite its complexity, different factors have been observed to influence the SST and extension of the IPWP, including (i) latitudinal shifts in the tropical rainbelt and its associated monsoonal winds, (ii) changes in the Indian and Pacific Walker circulations mostly through El Niño–Southern Oscillation (ENSO), and (iii) changes in the transport and/or properties of Pacific warm and fresh waters through the Indonesian Archipelago into the Indian Ocean. Next, we will introduce and discuss how these three climatic processes are interlinked and more specifically assess the role and response of the IPWP.

The Intertropical Convergent Zone (ITCZ) is a narrow tropical belt of wind convergence and maximum surface moist static energy, which is part of the ascending branch of the Hadley circulation. The position of the ITCZ is largely controlled by the latitudinal SST gradients governed by the seasonal distribution of incoming solar radiation, which drives the location of the ITCZ toward the summer hemisphere (Schneider et al., 2014). This seasonal migration modifies the IPWP shape and location as can be observed in the SST maps (Figure 1). The latitudinal migration of the rainbelt and the accompanying winds give rise to the Asian-Australian monsoons. Changes in the monsoonal activity affect the wind intensity and direction over the IPWP causing large seasonal differences in the local SST. Specifically, the Indian Ocean sector of the IPWP, comprising Timor, Arafura, and Banda Seas, is influenced by the seasonal reversal of the monsoonal winds which cause upwelling of colder waters through Ekman transport (Qu & Meyers, 2005; Kim et al., 2012; Jochen, 2015). The Pacific sector of the IPWP, such as around Papua New Guinea, also presents monsoonal upwelling-driven seasonal SST changes (Delcroix et al., 2014); however, the magnitude of these is smaller and mostly overridden by interannual changes related to ENSO variability (Kim et al., 2012). In addition, ENSO and the monsoons can also affect the freshwater input predominantly in the South China Sea, which can induce changes in the surface circulation and hence the strength of the ITF (e.g., Gordon et al., 2012).

ENSO variability across the tropical Pacific affects the SST and the areal extent and location of the IPWP. Coupled ocean-atmospheric changes redistribute the surface ocean heat between the western and eastern parts of the equatorial Pacific (Bjerknes, 1969; Fu et al., 1986; McPhaden & Picaut, 1990; Picaut et al., 1996; Yan et al., 1992). For instance, during El Niño years the easterly trades are weakened and the Pacific thermocline tilt is reduced which redistributes the ocean heat eastward resulting in colder temperatures than during background conditions, particularly in the Pacific sector of the IPWP (the WPWP). Conversely, La Niña years are often associated with warmer than average SST in the IPWP and a more stable tropical Pacific mean state. Model results suggest the important role of the Western Pacific in exciting ENSO variability (Palmer & Mansfield, 1984). Observational studies document cold winter SST in the IPWP, specifically, in the coast of Papua New Guinea, during six El Niño events between 1981 and 2005, and have been argued to precondition El Niño events (Hasegawa et al., 2009; Hasegawa et al., 2010).

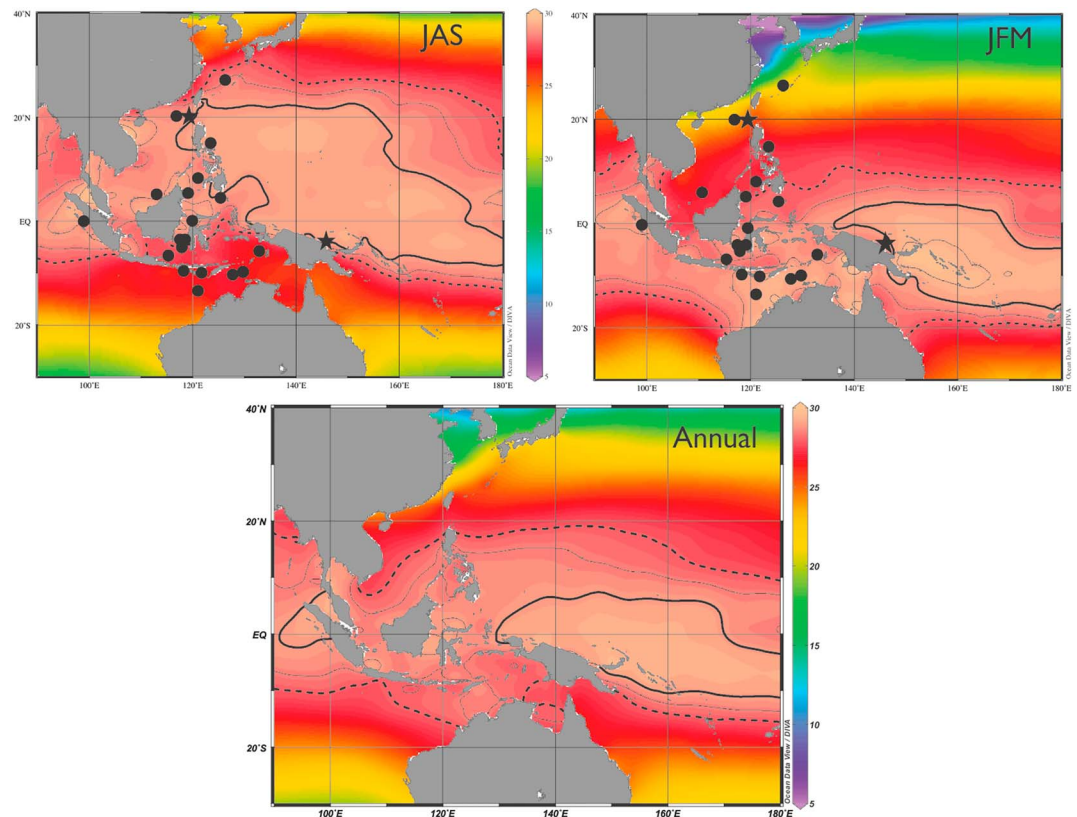


Figure 1. Boreal summer (July–September, top left panel), winter (January–March, top right panel), and annual sea surface temperatures of the Indo-Pacific Warm Pool region (1955–2013). Contours highlight temperatures above 28 °C at 0.5 °C increments (Locarnini et al., 2013; Schlitzer, 2015). Dashed contour indicates the 28 °C isotherm outlining the area often referred to as the IPWP, the solid contour outlines the area with temperatures >29 °C often referred to as the WPWP region. Previously published foraminiferal-based SST records (black circles) and new records (black stars) presented in this study are indicated on the seasonal maps.

In addition, ENSO modifies the surface ocean conditions not only zonally across the Pacific but also meridionally. During El Niño events, the bifurcation of the western tropical Pacific surface currents are found in a more northward position (Hu et al., 2015; Figure 2). In addition, the relaxation of the Pacific trade winds (Wyrtki, 1987) alters the circulation slowing and shoaling the transport from the Western Pacific into the Indonesian Archipelago (Sprintall et al., 2014) with a lesser proportion of warm waters from the South Pacific deriving from the New Guinea Coastal Current (van Sebille et al., 2014). Changes in the westward transport of warm water out of the Pacific into the Indian Ocean through the ITF can also affect the IPWP intensity and shape. Aside from ENSO, ITF transport variability has been found to be linked to seasonal monsoonal winds (Gordon et al., 2003), which regulate the presence of warmest waters within the western portion of the IPWP at the entrance passageways (Gordon & Fine, 1996) and the vertical mixing in the Maritime Continent (Sprintall et al., 2014). This variability in the surface ocean conditions can feed back into the coupled ocean-atmospheric dynamics in the tropical Pacific (England & Huang, 2005; Gordon et al., 2003; Koch-Larrouy et al., 2010; Oppo & Rosenthal, 2010).

Previous continuous high-resolution paleoceanographic studies spanning the last deglaciation and the Holocene mainly focus on reconstructing surface ocean conditions in the larger area of the IPWP (Figure 1), comprising regions such as (i) the western part of IPWP in the Indian Ocean side of the Indonesian Archipelago including Sumatra (Mohtadi et al., 2010; Mohtadi et al., 2014), Java (Mohtadi, Oppo, Steinke, et al., 2011), and Savu/Timor Sea (Gibbons et al., 2014; Holbourn et al., 2011; Levi et al., 2007; Xu et al., 2008); (ii) within the Indonesian Archipelago such as Sulu Sea (Rosenthal et al., 2003), Makassar Strait (Fan et al., 2013; Fan et al., 2018; Linsley et al., 2010; Schröder et al., 2016; Schröder et al., 2018; Visser et al., 2003), Banda Sea, and South of the Philippines (Stott et al., 2004); and (iii) the northern edge of the IPWP comprising South China Sea (e.g., Steinke et al., 2001b; Steinke et al., 2008; Steinke

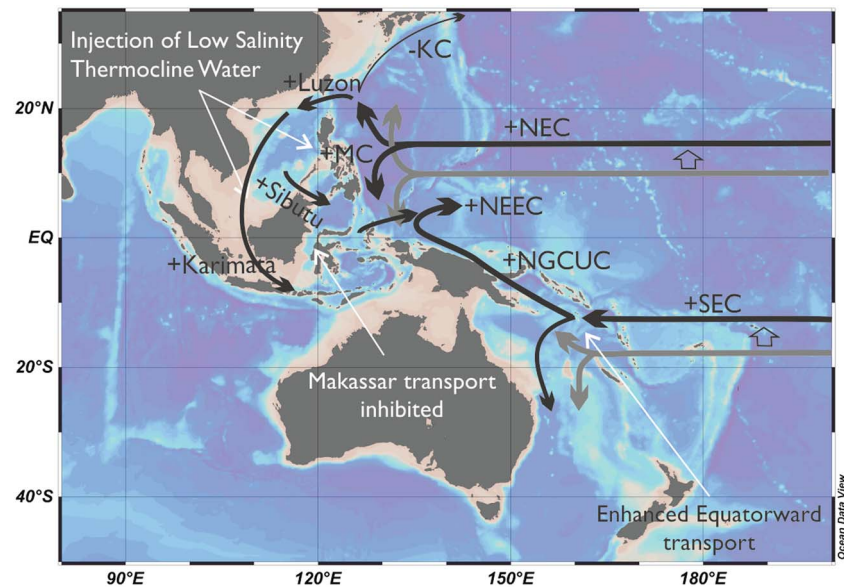


Figure 2. Surface ocean circulation schematics during El Niño events in black, normal conditions are indicated in grey, and empty arrows indicate northward migration (after Ganachaud et al., 2014; Hu et al., 2015). As described in the text the bifurcation of the boundary currents is shifted northward during El Niño events increasing the equatorward surface transport of the South Equatorial Current (SEC) via the North Guinea Coastal Undercurrent (NGCUC). The reversing in the currents out of the Indonesian Archipelago toward the east limits the transport of the NGCUC through the ITF enhancing the Northeast Equatorial Current (NEEC). An increase in the North Equatorial Current (NEC) results in an increase of these waters through the Luzon Strait into the South China Sea while decreasing the northern transport by the Kuroshio Current (KC). Bathymetric base map was created using Ocean Data View (Schlitzer, 2015).

et al., 2011), Northern Philippines (Dang et al., 2012), and Okinawa Trough (South of Japan; Sun et al., 2005). A compilation of the available foraminiferal SST records in 2010 highlighted the common trends comprising a 2–3 °C deglacial warming which peaked during the early Holocene and was followed by a gradual 0.5 °C cooling toward present (Linsley et al., 2010). The coherent regional signals were attributed to a westward shift and/or expansion of the WPWP during the early Holocene (Linsley et al., 2010). Since all of these locations, lie on the edges of the IPWP (Figure 1), it is not yet clear if this was a change in the IPWP location/coverage or perhaps an early Holocene intensification, in other words a warmer IPWP.

In this study, we aim to test the hypothesis that the early Holocene IPWP was warmer by reconstructing the SST variability in a more central location within the heart of the IPWP, also known as the WPWP, from a sediment core located off the northeast coast of Papua New Guinea (Figure 1). This location is less likely to be affected by changes in the size of the IPWP and also allows us to monitor the southern Pacific end-member of the waters feeding into the IPWP and ITF (Gordon, 1986; Gordon et al., 1992). Advantageously, the SST at this location are minimally affected by changes in the seasons (Figure 1), which will also aid to test the hypothesis that many of the IPWP proxy records are seasonally biased due to the changes in local insolation (Liu, Zhu, et al., 2014; Timmermann et al., 2014). We also present a new subcentennially resolved record from the SCS and include other recently published data in order to update the IPWP SST compilation by Linsley et al. (2010) and thus provide a more comprehensive and up-to-date view of the regionalism of these SST changes over the last 17 kyr.

2. Study Sites

Marine sediment core RR1313-23PC is located off the northeast coast of Papua New Guinea (Figure 1) and lies in the pathway of the northward flowing New Guinea Coastal Current (NGCC), which is fed by the westward flowing South Equatorial Current and becomes seasonally reversed in direction through changes in the wind direction with respect to the position of the tropical rainbelt (Delcroix et al., 2014). Further north, the waters from the NGCC join the Equatorial Counter Current, part of which will also flow westward into the Indonesian Archipelago contributing to the southern end-member waters to the Indonesian Throughflow. More generally, throughout the year, the surface waters from the east coast of Papua New Guinea lie within

Table 1
RR1313-23PC AMS ^{14}C Measurements and Calibrated Ages

UCIAMS laboratory code	Depth (cm)	^{14}C age (years)	Error (years)	Calendar ages 95% confidence interval (years BP)	Calendar ages (years BP)
154260	4.5	1845	±20	1,311–1,474	1,392.5
154261	48.5	3500	±20	3,325–3,446	3,385.5
154262	100.5	4210	±20	4,225–4,396	4,310.5
154263	156.5	5605	±25	5,911–6,098	6,004.5
146231	208.5	7620	±30	7,994–8,160	8,077
154264	260.5	9010	±25	9,547–9,805	9,676
170927	282.5	9430	±20	10,196–10,357	10,276.5
170928	330.5	10035	±25	10,900–11,153	11,026.5
170929	362.5	10715	±25	11,961–12,342	12,151.5
170930	430.5	12605	±25	13,966–14,201	14,083.5
170931	490.5	13075	±25	14,904–15,235	15,069.5
146232	544.5	13655	±45	15,745–16,105	15,925

the heart of the IPWP, in the WPWP (Figure 1), and are largely affected by its spatial extent, strength, and location, which is dependent on the westward movement of warm waters across the tropical Pacific as part of changes in ENSO.

Marine sediment ODP Site 1144 (ODP1144 hereafter) lies in the South China Sea (SCS), and hence on the northern boundary of the IPWP. As a marginal basin, hydrographic changes in the SCS predominantly governed by the seasonal reversal of wind direction/intensity associated with the East Asian Monsoon and to a lesser extent by the mixture of the inflow waters from the surrounding straits (Wang et al., 2014). As a result of the seasonal reversal in the atmospheric circulation the SCS experiences large seasonal changes in SST with uniform temperatures (28.5–29.5 °C) in the summer to steep latitudinal gradients (20.5–27.5 °C) in the winter (Figure 1).

3. Materials and Core Chronology

Marine sediment core RR1313-23PC (4.4939°S, 145.6703°E; 712-m water depth) was recovered in September 2013 during R/V *Roger Revelle* Cruise RR1313 and was sampled between - and 8-cm resolution equivalent to a minimum time resolution of approximately 80 years. The core chronology from RR1313-23PC (23PC hereafter) was established using 12 AMS radiocarbon dates measured on approximately 8–12 mg of sample material combination of *Globigerinoides ruber* and *Globigerinoides sacculifer* individuals (>250 μm test size fraction; Table 1). The radiocarbon dates were measured in the W.M. Keck Carbon Cycle Accelerator Mass Spectrometer Facility at the University of California, Irvine.

Ocean Drilling Program ODP1144 (20.053°N, 117.4189°E; water depth 2,037 m) is located in the Northeast SCS. The top 11 m of the core composite depth (mcd) were sampled at 5-cm resolution. The new SST record from ODP1144 record improves the resolution of the published SCS *G. ruber* record from MD01-2390 (Steinke et al., 2008) with an average temporal resolution of 68 years (between 20 and 100 years) enabling robust interpretation of some of the features from the northern boundary of the WPWP. The age model for the record from ODP1144 was produced using four radiocarbon dates presented in Bühring et al. (2004).

The radiocarbon ages from RR1313-23PC and ODP1144 were converted to calendar ages using MarineCal13, which includes a global ocean reservoir correction of 405 years, and we did not apply an additional reservoir correction (Reimer et al., 2013). The core chronologies were built using BChron package (Parnell et al., 2008) which uses Bayesian statistics in order to calculate the 90% probability error envelope of the age models (Figure 3).

4. Methodology

4.1. Planktonic Foraminifera Mg/Ca

For the SST reconstructions the surface dweller foraminiferal species *G. ruber sensu stricto* was used. Around 50 foraminiferal tests were selected from the 250–300-μm size fraction from core RR1313-23PC and 30–40 individuals from the 250–355-μm size fraction for ODP1144. The foraminiferal shells were translucent showing extraordinary preservation. These samples were lightly crushed between two glass plates in order to open up the chambers to aid the chemical cleaning of test fragments. The foraminiferal samples were cleaned using the full reductive and oxidative cleaning procedure (Boyle & Keigwin, 1985; Rosenthal et al., 1997). Samples were analyzed for Mg/Ca using Thermo Element ICPMS-XR at Rutgers University following the method of Rosenthal et al. (1999). The long-term precision of the instrument was <2% based on repeated analysis of a laboratory internal consistency standard (Mg/Ca = 3.3 mmol/mol) throughout the analysis periods (2007–2010 and 2014–2016). Potential contamination phase biases on the Mg/Ca values were assessed by comparing the Mg/Ca values against Fe/Ca, Mn/Ca, and Al/Ca, and these presented no downcore covariability indicative of minimal postdepositional alteration.

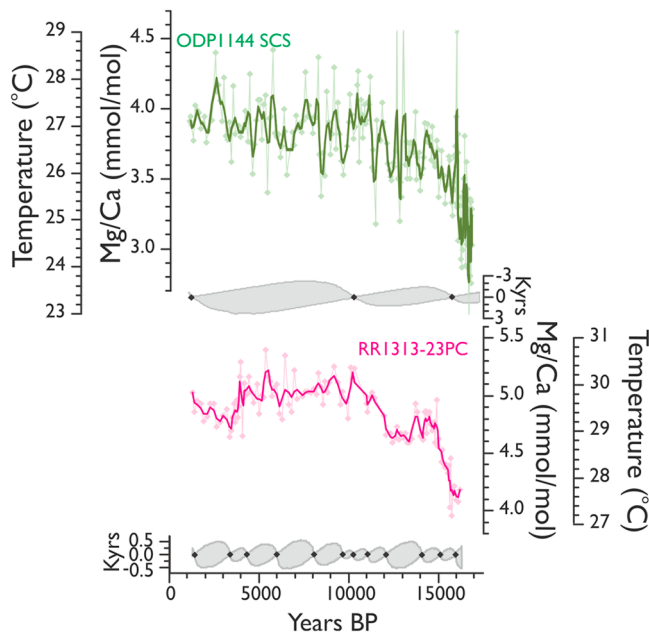


Figure 3. Foraminiferal Mg/Ca-derived surface ocean temperatures from ODP1144 in the South China Sea and RR1313-23PC from Papua New Guinea. Radiocarbon ages are presented in black diamonds and the age uncertainties (90% confidence) are shown as the grey shaded areas in kyr.

In RR1313-23PC, Fe/Ca, Mn/Ca, and Al/Ca values were typically around and/or below 0.1 mmol/mol; no covariance was found in the Fe/Mg, Mn/Mg, and Al/Mg around 0.03, 0.08, and 0.08 mol/mol, respectively. Following contaminant thresholds presented by Barker et al. (2003) these values indicate that the Mg/Ca values have not been affected by additional Mg-rich contaminant phases. Postdepositional dissolution was assessed by comparing the samples' average shell weight with the Mg/Ca, which revealed no significant correlation, and hence no dissolution of the original foraminiferal calcite. In core ODP1144, Mn/Ca values were typically 0.160 mmol/mol with values of around 0.3 mmol/mol between 673 and 913 mcd (13–16 kyr). Fe/Ca values were typically around 0.29 mol/mol and Al/Ca below 0.3 mmol/mol. Moreover, Fe/Mg and Mn/Mg yielded values of ~0.1 and 0.045 mmol/mmole, respectively. These results confirm the lack of contaminant phases in these samples that would affect the interpretation of the Mg/Ca as a temperature proxy.

The Mg/Ca ratios were converted to temperatures using the species specific *G. ruber* calibration by Anand et al. (2003); this calibration was chosen as it is consistent with regional calibrations from the IPWP (Hollstein et al., 2017; Mohtadi, Oppo, Lückge, et al., 2011; Zhang et al., 2018). Since the reductive step dissolves approximately 8–15% of the foraminiferal shell (Barker et al., 2003; Rosenthal et al., 2004), a 10% dissolution correction was applied to be comparable to the Anand et al. (2003) calibration study and convert Mg/Ca values to temperatures (Figure 3). The core-top Mg/Ca-derived temperatures from the companion multicore for 23PC reveal Mg/Ca values of 4.95 mmol/mol (equivalent to 29.8 °C), a value that is within the range of modern temperature measurements at the core site (Figure 1) and hence supporting the use of this calibration. It is important to note that the comparison between the new and published records is done by using the anomalies of the calculated SST with respect to a certain time period (as discussed in section 4.1) which will be unaffected by the cleaning correction samples underwent.

Nonthermal controls on Mg/Ca, such as salinity and carbonate chemistry, were documented to influence Mg incorporation into foraminiferal calcite since the beginning of planktonic foraminifera culturing experimentation (Lea et al., 1999; Nürnberg et al., 1996). Although, translating environmental sensitivities (e.g., salinity and carbonate chemistry) to Mg/Ca determined in culture to open ocean foraminifera is not necessarily straightforward. For example, large discrepancies in the sensitivity of foraminiferal Mg/Ca to salinity determined in culture studies (3–5%/psu; Hönsch et al., 2013; Kısakürek et al., 2008; Lea et al., 1999) were significantly lower than what was revealed by core-top studies (15–29%/psu; Arbuszewski et al., 2010; Ferguson et al., 2008; Mathien-Blard & Bassinot, 2009). Recent reevaluation of Mg/Ca sensitivity to salinity in *G. ruber* estimate 3.3–6.7%/psu in agreement with initial culture experiment estimates (Gray et al., 2018; Hertzberg & Schmidt, 2013; Hönsch et al., 2013). Notably, however, there is no discernible effect at salinities below 34 psu. At higher salinities, the lower salinity sensitivity estimate of $3.3 \pm 2.2\%/psu$ is based on globally compiled open ocean samples and likely is most comparable to downcore records. A regional multispecies core-top calibration found no significant correlation between the Mg/Ca values and salinity in the WPWP region which comprised a local variation of 1.5 (Hollstein et al., 2017; Zhang et al., 2018). Regional planktonic seawater $\delta^{18}O$ ($\delta^{18}O_{sw}$) records encompassing our sites exhibit minor variation ($<0.5\text{‰}$), signifying little change in surface salinity within the last 12,000 years (Gibbons et al., 2014). Dramatic changes in surface pH are also not expected as atmospheric CO_2 levels remain relatively constant over the Holocene. Based on these observations our Mg/Ca-based surface temperature reconstructions over the Holocene would be negligibly influenced by nonthermal controls of pH and salinity. However, absolute surface temperatures during the early deglaciation might be biased. In a recent assessment on the effects of surface salinity and pH variability on Mg/Ca-SST estimate a mean surface ocean overestimation of $<1.5\text{ °C}$ at the Last Glacial Maximum (LGM; Gray & Evans, 2019). Tropical surface waters are in near equilibrium with the atmosphere (Takahashi et al., 2017), and surface pH change ensued by an increase in atmospheric CO_2 would be expressed uniformly throughout the region. Regional variation in salinity based on model output

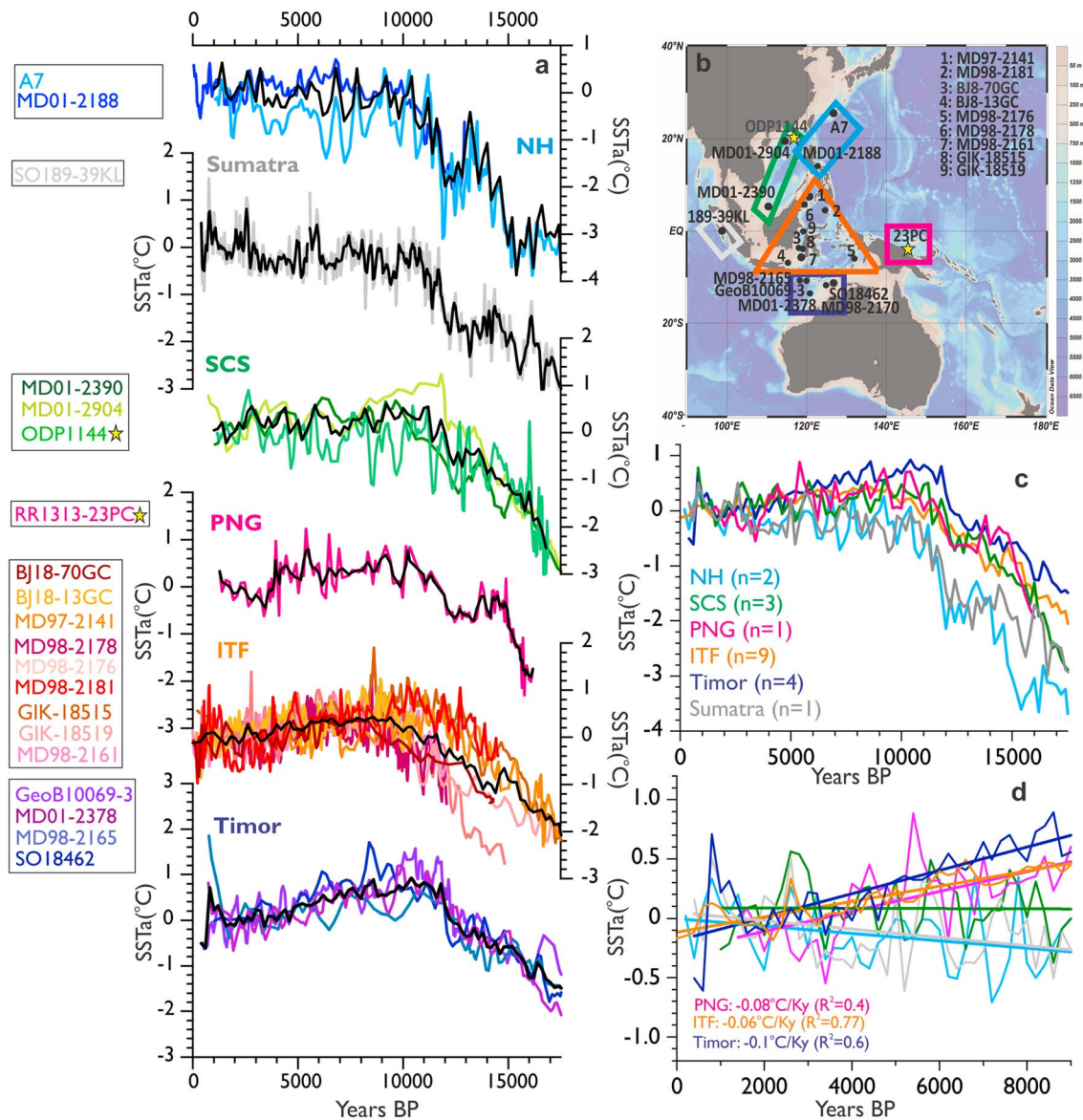


Figure 4. Regional SST anomaly reconstructions of the Indo-Pacific Warm Pool across the last 17,000 years. (a) New and published individual sea surface temperature records are grouped into five color-coded regions indicated in the map by the boxes (b). The regional averages are shown in black (note that the black lines are the 200-year interpolated regional averages except in the PNG and Sumatra records which is the weighted 3-point average). Northern Hemisphere (NH): Okinawa Trough (Sun et al., 2005), MD01-2188 (Dang et al., 2012); South China Sea (SCS): MD01-2390 (Steinke et al., 2008), MD01-2904 (Steinke et al., 2011), ODP1144 (this study); Sumatra: SO189-39KL (Mohtadi et al., 2014); Papua New Guinea (PNG): RR1313-23PC (this study); Indonesian Throughflow (ITF): BJ18-70GC/13GC (Linsley et al., 2010), MD97-2141 (Rosenthal et al., 2003), MD98-2176/81 (Stott et al., 2004), GIK185-19/15 (Schröder et al., 2016; Schröder et al., 2018), MD98-2178/2161 (Fan et al., 2013); Timor Sea: GeoB10069-3 (Gibbons et al., 2014), MD01-2378 (Xu et al., 2008), MD98-2165 (Levi et al., 2007), SO18462 (Holbourn et al., 2011). (b) Regional map showing the core locations for the published records in black dots and yellow stars indicating the new sea surface temperature records presented in this study; color boxes delimit the region with the cores included (modified from ocean data view; Schlitzer, 2015). (c) Regional color-coded linearly interpolated 200-year step averages over the last 17,000 years. (d) Linear trends of the sea surface temperatures over the last 9,000 years, slopes with significance values p and f below <0.005 and with R^2 values of >0.12 are shown.

suggests surface freshening in South China Sea and saltier waters in the Makassar Straits (ITF region Figure 4b; Gray & Evans, 2019). This result corresponds to an overestimation of LGM Mg/Ca-SST in SCS and underestimation in the Makassar Straits. However, deglacial proxy records reveal consistent freshening from the Younger Dryas toward the Holocene (e.g., Gibbons et al., 2014; Linsley et al., 2010; Tierney et al., 2012), although $\delta^{18}\text{O}_{\text{sw}}$ values, which are related to salinity, across the IPWP between LGM and Holocene remain unchanged (Gibbons et al., 2014). The latter differs from the model results (Gray & Evans, 2019). Furthermore, the compiled Mg/Ca-based temperatures broadly agrees with other deglaciation IPWP

temperature reconstructions based on alkenones and coral paleothermometry which estimate LGM-Holocene changes of 2–3 °C (Gagan et al., 2004; Figure 4a). The Indo-Pacific hydroclimate is inherently complex and warrants caution when considering the implications of these model results on Mg/Ca-SST. With improved local surface salinity reconstructions during the LGM the potential salinity bias on Mg/Ca can be better constrained yielding more robust absolute temperatures.

4.2. Compilation of SST Data

We compiled continuous Mg/Ca-based *G. ruber* (white) SST records with high temporal resolution (on average less than 200 years for the last 17,500 years) alongside the two new sea surface temperature records (ODP1144-SCS and RR1313-23PC-PNG; Figures 3 and 4a). The 200-year resolution limit was chosen in order to warrant a robust interpretation of the multicentennial and millennial variability. The IPWP SST records were grouped into the following regions outlined in Figure 4b: (1) Northern Hemisphere (include the sites that are further north and under the influence of the southward flowing Kuroshio Current which is part of the North Pacific Gyre), (2) the South China Sea, (3) Western Sumatra in the equatorial Indian Ocean, (4) Indonesian Throughflow region which includes cores within the Indonesian Archipelago, (5) Timor Sea which comprises the southernmost locations on the Indian Ocean side of the IPWP, and (6) Papua New Guinea, a location bathed by waters originating further south (transported by the New Guinea Coastal Current) and in the heart of the WPWP. The temperatures used were the same calculated in the published data as the different calibrations used in these studies did not differ considerably in the preexponential and exponential constants of the Mg/Ca paleothermometry equation. Temperature anomalies were calculated for each record with respect to their average temperatures between 1,000 and 2,000 years BP except for MD97-2141 (Rosenthal et al., 2003) for which we used the core-top value. This time interval was selected as all records contained data points during this time period (unlike the 0–1,000 years BP), and it eased visual comparison for trends to converge toward the late Holocene. The records were resampled by linear interpolation at a 200-year step, and an average curve was calculated for each region (Figures 4a–4c). Linear regression of the regional averages was taken from 0–9,000 years BP to study the IPWP Holocene temperature evolution in each region (Figure 4d). Note that records with low temporal resolution (higher than 200 years) across the 0–9,000-year BP period were excluded from the calculations in Figure 4d. The significance in the linear trends was assessed through the calculation of p and f values in addition to the R^2 of the linear regressions. The selection of the last 9,000 years was chosen first to avoid the early Holocene warming as the late stages of the deglaciation and second to avoid the potential confounding signals from the effects of late deglacial sea level rise and the consequent flooding of the Sunda Shelf around ~9,500 years BP (e.g., Linsley et al., 2010).

5. Results and Discussion

5.1. Regional Differences in the Magnitude and Trend of the IPWP Holocene Temperature Evolution

Our new record from the center of the IPWP, from Papua New Guinea (PNG), records a smooth warming transition at the onset of the Holocene with warm temperatures persisting through the Holocene thermal maximum followed by a gradual and mild cooling toward present of around 0.08 °C/kyr over the last 9,000 years (Figures 3, 4a, and 4d). This is an interesting finding, considering previous literature explained variability in the IPWP to be dominated by a warmer and more western location of the early Holocene IPWP compared to present (Linsley et al., 2010). This Holocene cooling trend is also found in the other southern IPWP regions, albeit of different magnitude. For example, a Holocene cooling of 0.06 °C/kyr is found in the ITF region; however, the largest cooling of the entire IPWP is found in the Timor Sea with average changes of 0.1 °C/kyr (Figures 4a and 4d). These three regions present p and f values of the linear regression between 0 and 9,000 years BP below 0.005, which indicates that the trends are statistically significant. In addition, the R^2 values are between 0.4 and 0.77 (Figure 4d). These trends are also present in other lower resolution reconstructions (>200 years) in these regions (e.g., Bolliet et al., 2011; Lea et al., 2000; Stott et al., 2004; Visser et al., 2003). Coral-based SST reconstructions from Papua New Guinea, Vanuatu, and the Great Barrier Reef show considerable variability but several corals record cold episodes (or temperatures similar to modern) during the early and middle Holocene (9,000–5,500 years BP; Abram et al., 2009; Beck et al., 1997; Corrège et al., 2000; Gagan et al., 1998; McCulloch et al., 1996). Furthermore, coral SST reconstructions suggest cooler conditions during periods of the middle Holocene in the southern edges of the

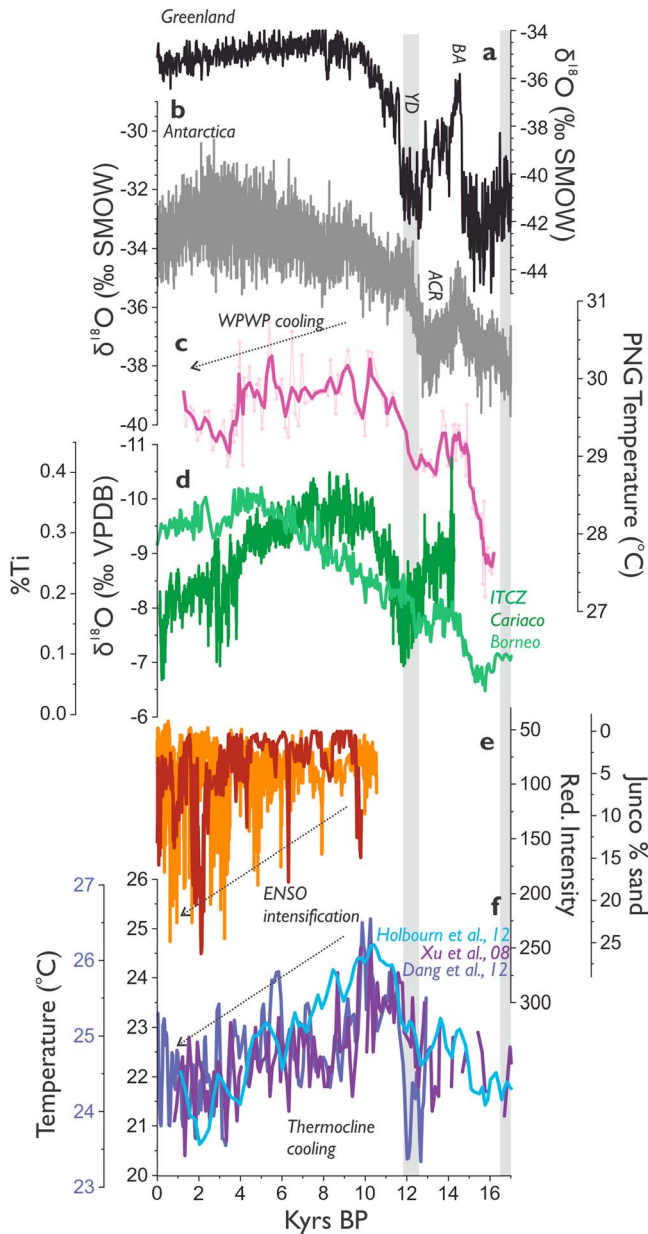


Figure 5. Ice core oxygen isotope reconstructions from (a) Greenland (NGRIP; Andersen et al., 2004) and (b) Antarctica EPICA Dronning Maud Land (EDML) ice core (Bazin et al., 2013). (c) SST reconstruction from Papua New Guinea (this study). (d) ITCZ hydrologic reconstructions based on relative percent titanium (Ti %) as an indicator of terrestrial runoff from the Cariaco Basin, located in the tropical Atlantic (Haug et al., 2001) and precipitation reconstruction based on $\delta^{18}\text{O}$ speleothem record from Borneo, Malaysia (Partin et al., 2007). (e) Changes in ENSO variability from % sand from El Junco lake, Galapagos (brown) (Conroy et al., 2008) and red color intensity (orange; Moy et al., 2002). (f) IPWP thermocline temperature reconstructions (Dang et al., 2012; Holbourn et al., 2011; Xu et al., 2008). Arrows highlight the approximate trends of the presented records.

IPWP (Abram et al., 2009) which differs from our findings (Figures 4a and 4d), and can perhaps be explained by the different frequency of ocean variability recorded in each proxy archive.

In contrast, the more northern region such as the Okinawa and Luzon Strait (NH; Dang et al., 2012; Sun et al., 2005), as well as a record off Sumatra in the eastern Indian Ocean (Mohtadi et al., 2014), do not present a predominant Holocene trend as shown in Figures 4a and 4d, and in the low R^2 values (<0.14) and high p and f values. The lack of a predominant Holocene trend is consistent with lower resolution records from this same region (Mohtadi et al., 2014; Setiawan et al., 2015).

The Mg/Ca-based records from the northern SCS show fairly constant temperatures over the Holocene particularly evident in the new record from ODP1144 (Figure 3) and MD01-2390 (Steinke et al., 2008), although the more southwestern lower resolution record from MD05-2904 (Steinke et al., 2011) shows a slight cooling over the Holocene (Figure 4a). These trends in the SCS agree with other reconstructions based on planktonic foraminiferal assemblages (Liu et al., 2013; Steinke et al., 2001a), however, markedly differ with alkenone-based temperature reconstructions from the SCS (mainly the organic proxy $U^{K'}_{37}$), which reveal a gradual warming of $\sim 2^\circ\text{C}$ between 6 and 11 kyr (Huang et al., 1997; Kienast et al., 2001; Pelejero et al., 1999; Zhao et al., 2006). These discrepancies are arguably attributed to different preferred living seasons of the proxy carriers (Mohtadi et al., 2010; Rosell-Melé & Prahl, 2013; Steinke et al., 2008; Timmermann et al., 2014) and possibly variations in habitat depth as the maximum production depth of haptophytes (alkenone proxy carriers) which can vary according to seasonal nutrient availability (Lohmann et al., 2013; Sachs et al., 2007), specifically implying changes in production of alkenones toward the summer months and/or a shallower maximum production depth between 6 and 11 kyr.

In the following sections we explore three different scenarios to explain the regional variations in the magnitude of the long-term trends at these sites: (i) southward shift in the latitudinal position of the tropical rainbelt, (ii) changes in the Walker circulation in the tropical Pacific associated with tropical Pacific mean climate state and ENSO variability, and (iii) changes in thermocline temperatures and/or the vertical mixing of the upper water column.

5.1.1. Latitudinal Shifts in the Intertropical Convergence Zone and Monsoonal Changes

Precession-driven decrease in Northern Hemisphere summer insolation from the early to late Holocene led to a gradual southward shift of the boreal-summer ITCZ position (Fleitmann et al., 2007; Haug et al., 2001; Wang et al., 2005). However, precipitation reconstructions from the Maritime Continent based on XRF in sedimentary cores (Kuhnt et al., 2015), $\delta^{18}\text{O}$ in speleothems from Flores (Griffiths et al., 2009) and Borneo (Partin et al., 2007; Figure 5d), and seawater $\delta^{18}\text{O}$ paint a more complex picture (Gibbons et al., 2014; Linsley et al., 2010, and references herein). To identify the temperature influence of a southward shift of the ITCZ to the spatial SST changes within the IPWP we use

modern boreal summer (July–September) and annual SST distribution as analogues to the early/middle and late Holocene, respectively (Figure 1). However, according to the seasonal latitudinal migration in Figure 1, the early/middle Holocene would have resulted in colder temperatures at the most southern regions transitioning to a warmer late Holocene and conversely a Holocene cooling on the more

northern sites. Furthermore, the new SST record from PNG lies at a location in which the SST are not affected by seasonal fluctuations in the ITCZ and hence would not show a trend if latitudinal migrations were the single cause of the Holocene IPWP trends. Since this is not what is observed in the reconstructions we therefore conclude that meridional shifts in the ITCZ alone cannot explain the Holocene regional SST patterns found in the data. However, ITCZ shifts would have been accompanied by the reorganization of atmospheric circulation and hence the monsoons potentially influencing the regional ocean conditions.

In the southern IPWP, the Australian-Indonesian Monsoon causes seasonal reversals in the wind direction from southeasterly to northwesterly winds in austral winter/summer, respectively. Because of the relative position of the coast with respect to the winds, the Ekman transport has profound effects on the local oceanography and upwelling off Java/Timor Sea. For instance, southeasterly monsoonal winds in austral winter (July-September) lead to strong northwest flow of the Java Current which drives upwelling of colder waters to the sea surface through offshore Ekman transport, whereas during the summer monsoon (January-March), this current is reversed and weakened (Quadfasel & Cresswell, 1992; Schott & McCreary, 2001). Similarly, the SCS is affected by the seasonal changes in the monsoonal winds with weak/strong northwesterlies leading to warm/cold SST conditions in boreal summer (July-September)/winter (January-March). Further east, off Papua New Guinea, the summer (July-September) northwesterly trade winds drive a southward transport of the NGCC and seasonal upwelling which in turn impacts SST along the coast of PNG and a shoaling of the 27 °C isotherm (Delcroix et al., 2014; Ueki et al., 2003). However, these changes in upwelling do not lead to large seasonal temperature changes, and hence, this region remains unique for its lack of seasonal SST variability.

The monsoons intensity and position have been shown to strongly respond to insolation over the Holocene (Kutzbach, 1981; Liu et al., 2003). Yet the monsoon strengthening recorded in SE Indonesia ahead of early Holocene insolation changes suggests that the sea level rise and the flooding of the Sunda Shelf enhanced the regional monsoon by increasing the moisture transport (Griffiths et al., 2009). The opening of the Karimata Strait allowed the warm and fresh SCS waters (Qu et al., 2006) to reach the southern Makassar Strait. Such surface ocean current reorganization in the ITF region could potentially explain the difference in timing of the early Holocene peak warming in the ITF records (Figure 4a). However, these do not show any coherent spatial pattern in the SSTs such as differences between the northern and southern Makassar Strait which is in agreement with previous work in this area (Linsley et al., 2010).

Proxy records from Java, located west of the Timor Sea region, show an enhanced early Holocene Australian-Indonesian Winter Monsoon leading to strong upwelling in this region (Mohtadi, Oppo, Steinke, et al., 2011). Thermocline records from the Timor Sea indicate warmer waters in the early Holocene (Xu et al., 2008; Holbourn et al., 2011; Figure 5f), which despite the upwelling may have resulted in warmer SST than the late Holocene (section 5.1.3). The combination between the differential effects of the reversing monsoonal winds on the upwelling and the underlying thermocline temperature patterns along the ITF route could explain the larger Holocene cooling trend found in the Timor Sea region (Figure 4).

5.1.2. Tropical Pacific Mean Climate State

The Holocene cooling within the center of the IPWP, as revealed by the new SST reconstructions from Papua New Guinea (Figure 3), is consistent with the reconstructed and modeled transition from an early middle Holocene predominant La Niña-like mean state or normal conditions toward a predominant late Holocene El Niño-like mean state (where the Pacific sector of the IPWP would be less intense and the warm waters would be redistributed across the equatorial Pacific; e.g., Clement et al., 2000; Liu et al., 2000). Holocene reconstructions sensitive to variation in ENSO based on lake sediments, corals, or single foraminifera oxygen isotope measurements document differing results on centennial-time scales in terms of ENSO variability and intensity, although most records broadly agree on a reduction of ENSO variability over the middle Holocene relative to the late Holocene (Carré et al., 2014; Chen et al., 2016; Cobb et al., 2013; Conroy et al., 2008; Koutavas et al., 2006; McGregor et al., 2013; McGregor & Gagan, 2004; Moy et al., 2002; Tudhope et al., 2001; White et al., 2018; Figure 5e). This is consistent with a more stable tropical Pacific Mean State (e.g., a more predominant La Niña-like state and larger tropical Pacific SST zonal gradient; Carré et al., 2012; Sadekov et al., 2013) with stronger trade winds and a more northerly position of the ITCZ (McGregor et al., 2008). The proxy data were successfully reproduced by a model study which attributed the Holocene ENSO intensification to orbital changes modulating the mean climate conditions and

changing the atmosphere-ocean feedback in the tropical Pacific (Liu, Lu, et al., 2014). Specifically, climate models have shown precessional effects on ENSO through changes in the zonal distribution of the winds and SST from meridional changes in the ITCZ (An, 2000; Clement et al., 1999; Clement et al., 2000; Liu et al., 2000), although alternative explanations suggest nonlinear ENSO responses to insolation (Emile-Geay et al., 2007; Timmermann et al., 2007) or stochastic forcings (Chiang et al., 2009). Other studies argue for no clear link between ENSO variability and insolation, and conclude that climate models are not capable of capturing the amplitude and/or timing of the ENSO variability shown in the proxy data (Emile-Geay et al., 2016). Yet, this could equally be due to the sparsity of high-resolution and temporally continuous paleoclimate data from the ENSO centers of action to accurately describe its variance. Our new SST reconstruction from Papua New Guinea suggests a warmer WPWP during the early/middle Holocene compared to the late Holocene likely associated with zonal displacements of the warm pool from changes in the tropical mean climate state in-line with model results (Tian et al., 2018). Furthermore, the SST record from Papua New Guinea shows a marked cooling between 3 and 4 kyr (Figure 5c) coincident with the increased precipitation in Borneo (Figure 5d) resulting from a strong ENSO during this period (Partin et al., 2007). This additional feature supports the influence of ENSO in the center of the IPWP to explain its Holocene variability. Yet the fact that the Holocene cooling was most felt in other southern IPWP regions and with different magnitudes, it implies that other climatic processes also played a role.

5.1.3. Changes in the Indonesian Throughflow and the Upper Water Column Structure

Regional changes in the upper water column structure via changes in the upper ocean heat content could have modified the SST. Available published thermocline temperature records from the Timor Sea (Holbourn et al., 2011; Xu et al., 2008), Mindanao (North Philippines; Dang et al., 2012), northern SCS (Steinke et al., 2011), and, off Papua New Guinea (Hollstein et al., 2018) consistently show early Holocene warming followed by a 2–3 °C gradual cooling toward the present (Figure 5f). Intermediate water temperatures in the Indonesian Throughflow region derived from North Pacific and southern sourced intermediate waters also show a similar long-term cooling over the Holocene (Rosenthal et al., 2013). The Holocene cooling deeper in the water column was potentially driven by high-latitude processes (Kalansky et al., 2015; Rosenthal et al., 2017), and consequently regionally expressed in the SST of the IPWP by upward mixing and thermal diffusion processes (e.g., Richards et al., 2012). It is therefore possible that the consistent Holocene cooling in the southern regions, most noticeably in the Timor Sea region, was a result of increased upward mixing of the cold waters via water mass transformation within the ITF region (i.e., the Banda Sea). Since the magnitude of cooling in the ITF SST reconstructions is of lesser magnitude than the Timor Sea (Figure 4) it is likely that the SST additionally responded to wind-driven upwelling as a response to changes in the Australian-Indonesian Winter Monsoon (section 5.1.1).

The Timor Sea region delimited in Figure 4b lies in the pathway of two main outflows of Indonesian Throughflow waters passing through the Ombai Strait and Timor Passage (accounting approximately for 80%) eventually reaching the Indian Ocean (Gordon, 2005; Sprintall et al., 2009). The Pacific waters that flow through the Indonesian Archipelago are considerably modified by vigorous vertical mixing by internal tidal waves and wind over the semienclosed Indonesian Seas, particularly around the Banda Sea (Field & Gordon, 1996; Hatayama, 2004; Koch-Larrooy et al., 2008; Koch-Larrooy et al., 2010). Changes either in the temperature of the thermocline waters transported into the Banda Sea from the Pacific and/or change in the intensity in the upward mixing of the thermocline in this region would have likely resulted in a cooling effect on the SST in the most southwest IPWP (Timor and ITF regions).

5.2. The Last Deglaciation in the Indo-Pacific Warm Pool

The mechanisms for glacial terminations and the abrupt climate variability superimposed on deglaciations are still a matter of much debate, initially because of the magnitude and abruptness of the climate variability in the North Atlantic and the proximity to continental ice sheets much of the research focused around this region. However, observations of early deglacial warming in the Southern Hemisphere and tropics (Lea et al., 2000; Visser et al., 2003) turned the spotlight to the tropics as a key player in deglaciations either by invoking internal tropical climate feedbacks (Clement et al., 1999, 2001) or through changes in tropical temperatures (Rodgers et al., 2003), likely in response to the increase in atmospheric CO₂ via deep-ocean degassing around Antarctica (Toggweiler & Lea, 2010). The temperature records from the IPWP remain equivocal, in terms of whether they are responding to the Northern Hemisphere abrupt climatic events (Kienast et al.,

2001), changes found in Antarctica (Lea et al., 2000; Stott et al., 2004; Visser et al., 2003), or a dual hemispheric response (Gibbons et al., 2014).

From the compiled data sets presented in Figures 4a and 4c we observe clear North Atlantic abrupt climate changes such as the Young Dryas cooling in the NH data. However, the Younger Dryas is less pronounced or absent in the Mg/Ca records from the SCS and Sumatra (Figures 4a and 4c). The relative proximity of these northern sites to the Asian Landmass makes them more sensitive to the ITCZ shifts as a response of the abrupt interhemispheric temperature changes during Northern Hemisphere cold events (Kienast et al., 2001). This restructuring of the Hadley circulation during the Younger Dryas and Heinrich Stadial 1 has been recorded in the hydrology records from the IPWP, chiefly foraminiferal $\delta^{18}\text{O}_{\text{sw}}$ records (Gibbons et al., 2014; Mohtadi et al., 2014) and in the stack of Chinese speleothems (Wang et al., 2008). Yet some hydroclimate records from the IPWP region reveal no presence of the high-latitude abrupt deglacial events (Partin et al., 2007; Partin et al., 2015; Figure 5d) raising questions about the response to remote versus local forcings (Partin et al., 2015). In contrast, the deglacial Northern Hemisphere signal (Figure 5a) is not as clear in the SST records across the IPWP which bear a different deglacial pattern, mostly recording a 2–3 °C gradual millennial warming (Figure 4a) and follow the deglacial changes in atmospheric CO_2 and the Antarctic gradual warming (Figure 5b). A deglacial hiatus in the warming around 12–14 kyr is present in our new record from PNG (Figure 5c) potentially related to the Antarctic Cold Reversal (Figure 5b). This is similarly found in the Timor Sea records (Figure 4a). This could either be linked to a Southern Ocean signal, transported at middepth through “ocean tunneling processes” into the tropical Pacific (Pena et al., 2008), or as a direct response to the global atmospheric CO_2 changes. Unfortunately, because of the lack of sufficiently fine age constraints in these records and the partial deglacial temporal coverage which does not include a full Heinrich Stadial 1, it is difficult to disentangle the northern versus the southern hemispheric deglacial abrupt climate change patterns from these data.

6. Conclusions

In this study we present two new SST records from the IPWP. One of the new sites is located in the heart of the IPWP (off Papua New Guinea), allowing for the first time to study the central and warmest waters of the IPWP across the last 17,000 years at subcentennial resolution. The new data are contextualized by comparing them to an updated regional SST compilation. Similarly to Linsley et al. (2010), our findings generally show a warm IPWP early Holocene period followed by a cooling trend toward the present. However, because of the improved spatial coverage of the records, we are able to identify that this cooling is mostly felt in the southern IPWP regions with spatially varying magnitude among them. We explore different potential explanations for the regionalism in the Holocene IPWP temperature evolution including changes in the position of the ITCZ and its associated monsoonal winds in conjunction with a cooling found in the thermocline waters and intensification of ENSO. We conclude that different regions were likely impacted differently by the proposed climatic processes resulting in the different magnitudes of variability. For instance, the large Timor Sea cooling likely resulted from the large impact of the reversing monsoonal winds driving upwelling of the cold underlying thermocline waters. We hypothesize that the smaller cooling trend recorded in PNG was more affected by ENSO-like changes across the tropical Pacific, whereas other regions such as the ITF and the southern SCS may have responded to a combination of several of these mechanisms. The late deglaciation (17,000–11,500 years) SST record from PNG shows similarities with the other IPWP SST reconstructions (except the NH records) with no clear presence of North Atlantic abrupt deglacial events. Instead, the IPWP SST shows a gradual deglacial surface warming in-line with the temperature changes in Antarctica and/or global atmospheric CO_2 . This feature could either suggest that the IPWP was responding either to the global atmospheric CO_2 rise or perhaps to hydrographic changes around the Southern Ocean propagated at middepths through the so-called “ocean tunneling” mechanism to the surface of the IPWP.

Acknowledgments

We would firstly like to thank the Editor and the two anonymous reviewers for providing comments which improved the manuscript. Thanks go to the crew and science party aboard of the R/V *Roger Revelle* Cruise RR1313, in particular to Gregory Mountain, for the recovery of the sediment marine core used in this study. We would also like to thank Dasha Gravilenko and Ryan Bu for laboratory assistance and Martina Hollstein for useful comments on the manuscript. This work was funded by NSF grant OCE1131371 to Y. Rosenthal. The data and calculations presented in this paper have been uploaded as a supporting information data file and stored in a data repository <https://doi.org/10.1594/PANGAEA.902662>.

References

- Abram, N. J., McGregor, H. V., Gagan, M. K., Hantoro, W. S., & Suwargadi, B. W. (2009). Oscillations in the southern extent of the Indo-Pacific Warm Pool during the mid-Holocene. *Quaternary Science Reviews*, 28(25–26), 2794–2803. <https://doi.org/10.1016/j.quascirev.2009.07.006>
- An, Z. (2000). The history and variability of the East Asian paleomonsoon climate. *Quaternary Science Reviews*, 19(1–5), 171–187. [https://doi.org/10.1016/S0277-3791\(99\)00060-8](https://doi.org/10.1016/S0277-3791(99)00060-8)

- Anand, P., Elderfield, H., & Conte, M. H. (2003). Calibration of Mg/Ca thermometry in planktonic foraminifera from a sediment trap time-series. *Paleoceanography*, *18*(2), 1050. <https://doi.org/10.1029/2002PA000846>
- Andersen, K. K., Azuma, N., Barnola, J. M., Bigler, M., Biscaye, P., Caillon, N., et al., & North Greenland Ice Core Project (2004). High-resolution record of Northern Hemisphere climate extending into the last interglacial period. *Nature*, *431*(7005), 147–151. <https://doi.org/10.1038/nature02805>
- Arbuszewski, J., de Menocal, P., Kaplan, A., & Farmer, E. C. (2010). On the fidelity of shell-derived $\delta^{18}\text{O}$ seawater estimates. *Earth and Planetary Science Letters*, *300*(3–4), 185–196. <https://doi.org/10.1016/j.epsl.2010.10.035>
- Barker, S., Greaves, M., & Elderfield, H. (2003). A study of cleaning procedures used for foraminiferal Mg/Ca paleothermometry. *Geophysics Geochemistry Geosystems*, *4*(9), 8407. <https://doi.org/10.1029/2003GC000559>
- Bazin, L., Landais, A., Lemieux-Dudon, B., Toyé Mahamadou Kele, H., Veres, D., Parrenin, F., et al. (2013). An optimized multi-proxy, multi-site Antarctic ice and gas orbital chronology (AICC2012): 120–800 ka. *Climate of the Past*, *9*(4), 1715–1731. <https://doi.org/10.5194/cp-9-1715-2013>
- Beck, J. W., Récy, J., Taylor, F., Edwards, R. L., & Cabioch, G. (1997). Abrupt changes in early Holocene tropical sea surface temperature derived from coral records. *Nature*, *385*(6618), 705–707. <https://doi.org/10.1038/385705a0>
- Bjerknes, J. (1969). Atmospheric teleconnections from the equatorial Pacific. *Monthly Weather Review*, *97*(3), 163–172. [https://doi.org/10.1175/1520-0493\(1969\)097<0163:ATFTEP>2.3.CO;2](https://doi.org/10.1175/1520-0493(1969)097<0163:ATFTEP>2.3.CO;2)
- Bolliet, T., Holbourn, A., Kuhnt, W., Laj, C., Kissel, C., Beaufort, L., et al. (2011). Mindanao Dome variability over the last 160 kyr: Episodic glacial cooling of the West Pacific Warm Pool. *Paleoceanography*, *26*, PA1208. <https://doi.org/10.1029/2010PA001966>
- Boyle, E. A., & Keigwin, L. D. (1985). Comparison of Atlantic and Pacific paleochemical records for the last 250,000 years: Changes in deep ocean circulation and chemical inventories. *Earth and Planetary Science Letters*, *76*(1–2), 135–150. [https://doi.org/10.1016/0012-821X\(85\)90154-2](https://doi.org/10.1016/0012-821X(85)90154-2)
- Bühring, C., Sarnthein, M., & Erlenkeuser, H. (2004). Toward a high-resolution stable isotope stratigraphy of the last 1.1 m.y.: Site 1144, South China Sea. In W. L. Prell, P. Wang, P. Blum, D. K. Rea, & S. C. Clemens (Eds.), *Proceedings of the Ocean Drilling Program, Scientific Results* (Vol. 184, pp. 1–29). College Station, TX: Ocean Drilling Program. <https://doi.org/10.2973/odp.proc.sr.184.205.2004>
- Carré, M., Azzoug, M., Bentaleb, I., Chase, B. M., Fontugne, M., Jackson, D., et al. (2012). Mid-Holocene mean climate in the south eastern Pacific and its influence on South America. *Quaternary International*, *253*, 55–66. <https://doi.org/10.1016/j.quaint.2011.02.004>
- Carré, M., Sachs, J. P., Purca, S., Schauer, A. J., Braconnot, P., Falcon, R. A., et al. (2014). Holocene history of ENSO variance and asymmetry in the eastern tropical Pacific. *Science*, *345*(6200), 1045–1048. <https://doi.org/10.1126/science.1252220>
- Chen, S., Hoffmann, S. S., Lund, D. C., Cobb, K. M., Emile-Geay, J., & Adkins, J. F. (2016). A high-resolution speleothem record of western equatorial Pacific rainfall: Implications for Holocene ENSO evolution. *Earth and Planetary Science Letters*, *442*, 61–71. <https://doi.org/10.1016/j.epsl.2016.02.050>
- Chiang, J. C. H., Fang, Y., & Chang, P. (2009). Pacific Climate Change and ENSO Activity in the Mid-Holocene. *Journal of Climate*, *22*(4), 923–939.
- Clement, A. C., Cane, M. A., & Seager, R. (2001). An orbitally driven tropical source for abrupt climate change. *Journal of Climate*, *14*(11), 2369–2375. [https://doi.org/10.1175/1520-0442\(2001\)014<2369:AODTSF>2.0.CO;2](https://doi.org/10.1175/1520-0442(2001)014<2369:AODTSF>2.0.CO;2)
- Clement, A. C., Seager, R., & Cane, M. A. (1999). Orbital controls on the tropical climate. *Paleoceanography*, *14*(4), 441–456. <https://doi.org/10.1029/1999PA900013>
- Clement, A. C., Seager, R., & Cane, M. A. (2000). Suppression of El Niño during the Mid-Holocene by changes in the Earth's orbit. *Paleoceanography*, *15*(6), 731–737. <https://doi.org/10.1029/1999PA000466>
- Cobb, K. M., Westphal, N., Sayani, H. R., Watson, J. T., Di Lorenzo, E., Cheng, H., et al. (2013). Highly variable El Niño–Southern Oscillation throughout the Holocene. *Science*, *339*(6115), 67–70. <https://doi.org/10.1126/science.1228246>
- Conroy, J. L., Overpeck, J. T., Cole, J. E., Shanahan, T. M., & Steinitz-Kannan, M. (2008). Holocene changes in eastern tropical Pacific climate inferred from a Galápagos lake sediment record. *Quaternary Science Reviews*, *27*(11–12), 1166–1180. <https://doi.org/10.1016/j.quascirev.2008.02.015>
- Corrège, T., Delcroix, T., Récy, J., Beck, W., Cabioch, G., & Le Cornec, F. (2000). Evidence for stronger El Niño–Southern Oscillation (ENSO) Events events in a Midmid-Holocene massive coral. *Paleoceanography*, *15*(4), 465–470. <https://doi.org/10.1029/1999PA000409>
- Cravatte, S., Delcroix, T., Zhang, D., McPhaden, M., & Leloup, J. (2009). Observed freshening and warming of the western Pacific warm pool. *Climate Dynamics*, *33*(4), 565–589. <https://doi.org/10.1007/s00382-009-0526-7>
- Dang, H., Jian, Z., Bassinot, F., Qiao, P., & Cheng, X. (2012). Decoupled Holocene variability in surface and thermocline water temperatures of the Indo-Pacific Warm Pool. *Geophysical Research Letters*, *39*, L01701. <https://doi.org/10.1029/2011gl050154>
- Delcroix, T., Radenac, M.-H., Cravatte, S., Alory, G., Gourdeau, L., Léger, F., et al. (2014). Sea surface temperature and salinity seasonal changes in the western Solomon and Bismarck Seas. *Journal of Geophysical Research: Oceans*, *119*, 2642–2657. <https://doi.org/10.1002/2013jc009733>
- Durack, P. J., Wijffels, S. E., & Matear, R. J. (2012). Ocean Salinities reveal strong global water cycle intensification during 1950 to 2000. *Science*, *336*(6080), 455–458. <https://doi.org/10.1126/science.1212222>
- Emile-Geay, J., Cane, M., Seager, R., Kaplan, A., & Almasi, P. (2007). El Niño as a mediator of the solar influence on climate. *Paleoceanography*, *22*, PA3210. <https://doi.org/10.1029/2006PA001304>
- Emile-Geay, J., Cobb, K. M., Carré, M., Braconnot, P., Leloup, J., Zhou, Y., et al. (2016). Links between tropical Pacific seasonal, interannual and orbital variability during the Holocene. *Nature Geoscience*, *9*(2), 168–173. <https://doi.org/10.1038/ngeo2608>
- England, M. H., & Huang, F. (2005). On the interannual variability of the Indonesian Throughflow and its linkage with ENSO. *Journal of Climate*, *18*(9), 1435–1444. <https://doi.org/10.1175/jcli3322.1>
- Fan, W., Jian, Z., Bassinot, F., & Chu, Z. (2013). Holocene centennial-scale changes of the Indonesian and South China Sea throughflows: Evidences from the Makassar Strait. *Global and Planetary Change*, *111*, 111–117. <https://doi.org/10.1016/j.gloplacha.2013.08.017>
- Fan, W., Jian, Z., Chu, Z., Dang, H., Wang, Y., Bassinot, F., et al. (2018). Variability of the Indonesian Throughflow in the Makassar Strait over the last 30 ka. *Scientific Reports*, *8*(1), 5678. <https://doi.org/10.1038/s41598-018-24055-1>
- Ferguson, J. E., Henderson, G. M., Kucera, M., & Rickaby, R. E. M. (2008). Systematic change of foraminiferal Mg/Ca ratios across a strong salinity gradient. *Earth and Planetary Science Letters*, *265*, 153–166. <https://doi.org/10.1016/j.epsl.2007.10.011>
- Ffield, A., & Gordon, A. L. (1996). Tidal mixing signatures in the Indonesian Seas. *Journal of Physical Oceanography*, *26*(9), 1924–1937. [https://doi.org/10.1175/1520-0485\(1996\)026<1924:TMSITI>2.0.CO;2](https://doi.org/10.1175/1520-0485(1996)026<1924:TMSITI>2.0.CO;2)
- Fleitmann, D., Burns, S. J., Mangini, A., Mudelsee, M., Kramers, J., Villa, I., et al. (2007). Holocene ITCZ and Indian monsoon dynamics recorded in stalagmites from Oman and Yemen (Socotra). *Quaternary Science Reviews*, *26*(1–2), 170–188. <https://doi.org/10.1016/j.quascirev.2006.04.012>

- Fu, C., Diaz, H. F., & Fletcher, J. O. (1986). Characteristics of the response of sea surface temperature in the central Pacific associated with warm episodes of the Southern Oscillation. *Monthly Weather Review*, *114*(9), 1716–1739.
- Fu, R., del Genio, A. D., & Rossow, W. B. (1994). Influence of ocean surface conditions on atmospheric vertical thermodynamic structure and deep convection. *Journal of Climate*, *7*(7), 1092–1108. [https://doi.org/10.1175/1520-0442\(1994\)007<1092:IOOSCO>2.0.CO;2](https://doi.org/10.1175/1520-0442(1994)007<1092:IOOSCO>2.0.CO;2)
- Gagan, M. K., Ayliffe, L. K., Hopley, D., Cali, J. A., Mortimer, G. E., Chappell, J., et al. (1998). Temperature and surface-ocean water balance of the mid-Holocene Tropical Western Pacific. *Science*, *279*(5353), 1014–1018. <https://doi.org/10.1126/science.279.5353.1014>
- Gagan, M. K., Hendy, E. J., Haberle, S. G., & Hantoro, W. S. (2004). Post-glacial evolution of the Indo-Pacific Warm Pool and El Niño–Southern oscillation. *Quaternary International*, *118–119*, 127–143. [https://doi.org/10.1016/s1040-6182\(03\)00134-4](https://doi.org/10.1016/s1040-6182(03)00134-4)
- Ganachaud, A., Cravatte, S., Melet, A., Schiller, A., Holbrook, N. J., Sloyan, B. M., et al. (2014). The Southwest Pacific Ocean circulation and climate experiment (SPICE). *Journal of Geophysical Research: Oceans*, *119*, 7660–7686. <https://doi.org/10.1002/2013jc009678>
- Gibbons, F. T., Oppo, D. W., Mohtadi, M., Rosenthal, Y., Cheng, J., Liu, Z., & Linsley, B. K. (2014). Deglacial $\delta^{18}\text{O}$ and hydrologic variability in the tropical Pacific and Indian Oceans. *Earth and Planetary Science Letters*, *387*, 240–251. <https://doi.org/10.1016/j.epsl.2013.11.032>
- Gordon, A. (2005). Oceanography of the Indonesian Seas and their throughflow. *Oceanography*, *18*(4), 13. <https://doi.org/10.5670/oceanog.2005.18>
- Gordon, A. L. (1986). Inter-ocean exchange of thermocline water. *Journal of Geophysical Research*, *91*(C4), 5037–5046. <https://doi.org/10.1029/JC091iC04p05037>
- Gordon, A. L., & Fine, R. A. (1996). Pathways of water between the Pacific and Indian Oceans in the Indonesian seas. *Nature*, *379*(6561), 146–149. <https://doi.org/10.1038/379146a0>
- Gordon, A. L., Huber, B. A., Metzger, E. J., Susanto, R. D., Hurlburt, H. E., & Adi, T. R. (2012). South China Sea throughflow impact on the Indonesian throughflow. *Geophysical Research Letters*, *39*, L11602. <https://doi.org/10.1029/2012gl052021>
- Gordon, A. L., Susanto, R. D., & Vranes, K. (2003). Cool Indonesian Throughflow as a consequence of restricted surface layer flow. *Nature*, *425*(6960), 824–828. <https://doi.org/10.1038/nature02038>
- Gordon, A. L., Weiss, R. F., Smethie, W. M., & Warner, M. J. (1992). Thermocline and intermediate water communication between the South Atlantic and Indian Oceans. *Journal of Geophysical Research*, *97*(C5), 7223–7240. <https://doi.org/10.1029/92jc00485>
- Gray, W. R., & Evans, D. (2019). Non-thermal influences on Mg/Ca in planktonic foraminifera: A review of culture studies and application to the Last Glacial Maximum. *Paleoceanography and Paleoclimatology*, *34*, 306–315. <https://doi.org/10.1029/2018pa003517>
- Gray, W. R., Weldeab, S., Lea, D. W., Rosenthal, Y., Gruber, N., Donner, B., & Fischer, G. (2018). The effects of temperature, salinity, and the carbonate system on Mg/Ca in *Globigerinoides ruber* (white): A global sediment trap calibration. *Earth and Planetary Science Letters*, *482*, 607–620. <https://doi.org/10.1016/j.epsl.2017.11.026>
- Griffiths, M. L., Drysdale, R. N., Gagan, M. K., Zhao, J.-X., Ayliffe, L. K., Hellstrom, J. C., et al. (2009). Increasing Australian–Indonesian monsoon rainfall linked to early Holocene sea-level rise. *Nature Geoscience*, *2*(9), 636–639. <https://doi.org/10.1038/ngeo605>
- Hasegawa, T., Ando, K., Mizuno, K., & Lukas, R. (2009). Coastal upwelling along the north coast of Papua New Guinea and SST cooling over the Pacific warm pool: A case study for the 2002/03 El Niño event. *Journal of Oceanography*, *65*(6), 817–833. <https://doi.org/10.1007/s10872-009-0068-y>
- Hasegawa, T., Ando, K., Mizuno, K., Lukas, R., Taguchi, B., & Sasaki, H. (2010). Coastal upwelling along the north coast of Papua New Guinea and El Niño events during 1981–2005. *Ocean Dynamics*, *60*(5), 1255–1269. <https://doi.org/10.1007/s10236-010-0334-y>
- Hatayama, T. (2004). Transformation of the Indonesian throughflow water by vertical mixing and its relation to tidally generated internal waves. *Journal of Oceanography*, *60*(3), 569–585. <https://doi.org/10.1023/B:JOCE.0000038350.32155.cb>
- Haug, G. H., Konrad, A. H., Sigman, D. M., Peterson, L. C., & Rohl, U. (2001). Southward migration of the Intertropical Convergence Zone through the Holocene. *Science*, *293*(5533), 1304–1308. <https://doi.org/10.1126/science.1059725>
- Hertzberg, J. E., & Schmidt, M. W. (2013). Refining *Globigerinoides ruber* Mg/Ca paleothermometry in the Atlantic Ocean. *Earth and Planetary Science Letters*, *383*, 123–133. <https://doi.org/10.1016/j.epsl.2013.09.044>
- Holbourn, A., Kuhnt, W., & Xu, J. (2011). Indonesian Throughflow variability during the last 140 ka: The Timor Sea outflow. *Geological Society, London, Special Publications*, *355*(1), 283–303. <https://doi.org/10.1144/SP355.14>
- Hollstein, M., Mohtadi, M., Rosenthal, Y., Moffa Sanchez, P., Oppo, D., Martínez Méndez, G., et al. (2017). Stable oxygen isotopes and Mg/Ca in planktonic foraminifera from modern surface sediments of the Western Pacific Warm Pool: Implications for thermocline reconstructions. *Paleoceanography*, *32*, 1174–1194. <https://doi.org/10.1002/2017pa003122>
- Hollstein, M., Mohtadi, M., Rosenthal, Y., Prange, M., Oppo, D. W., Martínez Méndez, G., et al. (2018). Variations in Western Pacific Warm Pool surface and thermocline conditions over the past 110,000 years: Forcing mechanisms and implications for the glacial Walker circulation. *Quaternary Science Reviews*, *201*, 429–445. <https://doi.org/10.1016/j.quascirev.2018.10.030>
- Hönisch, B., Allen, K. A., Lea, D. W., Spero, H. J., Eggins, S. M., Arbuszewski, J., et al. (2013). The influence of salinity on Mg/Ca in planktonic foraminifera—Evidence from cultures, core-top sediments and complementary $\delta^{18}\text{O}$. *Geochimica et Cosmochimica Acta*, *121*, 196–213. <https://doi.org/10.1016/j.gca.2013.07.028>
- Hu, D., Wu, L., Cai, W., Gupta, A. S., Ganachaud, A., Qiu, B., et al. (2015). Pacific western boundary currents and their roles in climate. *Nature*, *522*(7556), 299–308. <https://doi.org/10.1038/nature14504>
- Huang, C.-Y., Wu, S.-F., Zhao, M., Chen, M.-T., Wang, C.-H., Tu, X., & Yuan, P. B. (1997). Surface ocean and monsoon climate variability in the South China Sea since the last glaciation. *Marine Micropaleontology*, *32*(1–2), 71–94. [https://doi.org/10.1016/S0377-8398\(97\)00014-5](https://doi.org/10.1016/S0377-8398(97)00014-5)
- IPCC (2013). Climate Change 2013: The Physical Science Basis. In T. F. Stocker et al. (Eds.), *Contribution of Working Group I to the Fifth Assessment Report of the Intergovernmental Panel on Climate Change* (Chap. 14). Cambridge, United Kingdom and New York, NY, USA: Cambridge University Press.
- Jochen, J. (2015). Undercurrent-driven upwelling in the northwestern Arafura Sea. *Geophysical Research Letters*, *42*, 9362–9368. <https://doi.org/10.1002/2015GL066163>
- Kalansky, J., Rosenthal, Y., Herbert, T., Bova, S., & Altabet, M. (2015). Southern Ocean contributions to the eastern equatorial Pacific heat content during the Holocene. *Earth and Planetary Science Letters*, *424*, 158–167. <https://doi.org/10.1016/j.epsl.2015.05.013>
- Kienast, M., Steinke, S., Statterger, K., & Calvert, S. E. (2001). Synchronous tropical South China Sea SST change and Greenland warming during deglaciation. *Science*, *291*(5511), 2132–2134. <https://doi.org/10.1126/science.1057131>
- Kim, S. T., Yu, J.-Y., & Lu, M.-M. (2012). The distinct behaviors of Pacific and Indian Ocean warm pool properties on seasonal and inter-annual time scales. *Journal of Geophysical Research*, *117*, D05128. <https://doi.org/10.1029/2011jd016557>
- Kisakürek, B., Eisenhauer, A., Böhm, F., Garbe-Schönberg, D., & Erez, J. (2008). Controls on shell Mg/Ca and Sr/Ca in cultured planktonic foraminifera, *Globigerinoides ruber* (white). *Earth and Planetary Science Letters*, *273*(3–4), 260–269. <https://doi.org/10.1016/j.epsl.2008.06.026>

- Koch-Larrouy, A., Lengaigne, M., Terray, P., Madec, G., & Masson, S. (2010). Tidal mixing in the Indonesian Seas and its effect on the tropical climate system. *Climate Dynamics*, *34*(6), 891–904. <https://doi.org/10.1007/s00382-009-0642-4>
- Koch-Larrouy, A., Madec, G., Iudicone, D., Atmadipoera, A., & Molcard, R. (2008). Physical processes contributing to the water mass transformation of the Indonesian Throughflow. *Ocean Dynamics*, *58*(3–4), 275–288. <https://doi.org/10.1007/s10236-008-0154-5>
- Koutavas, A., de Menocal, P. B., Olive, G. C., & Lynch-Stieglitz, J. (2006). Mid-Holocene El Niño–Southern Oscillation (ENSO) attenuation revealed by individual foraminifera in eastern tropical Pacific sediments. *Geology*, *34*(12), 993–996. <https://doi.org/10.1130/G22810A.22811>
- Kuhnt, W., Holbourn, A., Xu, J., Opdyke, B., De Deckker, P., Röhl, U., & Mudelsee, M. (2015). Southern Hemisphere control on Australian monsoon variability during the late deglaciation and Holocene. *Nature Communications*, *6*, 5916.
- Kutzbach, J. E. (1981). Monsoon climate of the early Holocene: Climate experiment with the Earth's orbital parameters for 9,000 years ago. *Science*, *214*(4516), 59–61. <https://doi.org/10.1126/science.214.4516.59>
- Lea, D. W., Mashiotto, T. A., & Spero, H. J. (1999). Controls on magnesium and strontium uptake in planktonic foraminifera determined by live culturing. *Geochimica et Cosmochimica Acta*, *63*(16), 2369–2379. [https://doi.org/10.1016/S0016-7037\(99\)00197-0](https://doi.org/10.1016/S0016-7037(99)00197-0)
- Lea, D. W., Pak, D. K., & Spero, H. (2000). Climate impact of late Quaternary equatorial Pacific sea surface temperature variations. *Science*, *289*(5485), 1719–1724. <https://doi.org/10.1126/science.289.5485.1719>
- Levi, C., Labeyrie, L., Bassinot, F., Guichard, F., Cortijo, E., Waelbroeck, C., et al. (2007). Low-latitude hydrological cycle and rapid climate changes during the last deglaciation. *Geochemistry, Geophysics, Geosystems*, *8*, Q05N12. <https://doi.org/10.1029/2006GC001514>
- Linsley, B. K., Rosenthal, Y., & Oppo, D. W. (2010). Evolution of the Indonesian Throughflow and Western Pacific Warm Pool during the Holocene. *Nature Geoscience*, *3*, 578–583. <https://doi.org/10.1038/ngeo1920>
- Liu, J., Li, T., Xiang, R., Chen, M., Yan, W., Chen, Z., & Liu, F. (2013). Influence of the Kuroshio Current intrusion on Holocene environmental transformation in the South China Sea. *The Holocene*, *23*(6), 850–859. <https://doi.org/10.1177/0959683612474481>
- Liu, Z., Kutzbach, J., & Wu, L. (2000). Modeling climate shift of El Niño variability in the Holocene. *Geophysical Research Letters*, *27*(15), 2265–2268. <https://doi.org/10.1029/2000gl011452>
- Liu, Z., Lu, Z., Wen, X., Otto-Bliesner, B. L., Timmermann, A., & Cobb, K. M. (2014). Evolution and forcing mechanisms of El Niño over the past 21,000 years. *Nature*, *515*(7528), 550–553. <https://doi.org/10.1038/nature13963>
- Liu, Z., Otto-Bliesner, B., Kutzbach, J., Li, L., & Shields, C. (2003). Coupled climate simulation of the evolution of global monsoons in the Holocene. *Journal of Climate*, *16*(15), 2472–2490. [https://doi.org/10.1175/1520-0442\(2003\)016<2472:CCSOTE>2.0.CO;2](https://doi.org/10.1175/1520-0442(2003)016<2472:CCSOTE>2.0.CO;2)
- Liu, Z., Zhu, J., Rosenthal, Y., Zhang, X., Otto-Bliesner, B. L., Timmermann, A., et al. (2014). The Holocene temperature conundrum. *Proceedings of the National Academy of Sciences*, *111*(34), E3501–E3505. <https://doi.org/10.1073/pnas.1407229111>
- Locarnini, R. A., Mishonov, A. V., Antonov, J. I., Boyer, T. P., Garcia, H. E., Baranova, O. K., et al. (2013). *World Ocean Atlas 2013. Volume 1: Temperature*, S. Levitus, Ed., A. Mishonov Technical Ed., NOAA Atlas NESDIS (Vol. 73, 40 pp.). Washington DC: U.S. Government Printing Office.
- Lohmann, G., Pfeiffer, M., Laepple, T., Leduc, G., & Kim, J.-H. (2013). A model-data comparison of the Holocene global sea surface temperature evolution. *Climate of the Past*, *9*(4), 1807–1839. <https://doi.org/10.5194/cp-9-1807-2013>
- Marcott, S. A., Shakun, J. D., Clark, P. U., & Mix, A. C. (2013). A reconstruction of regional and global temperature for the past 11,300 years. *Science*, *339*(6124), 1198–1201. <https://doi.org/10.1126/science.1228026>
- Marsicek, J., Shuman, B. N., Bartlein, P. J., Shafer, S. L., & Brewer, S. (2018). Reconciling divergent trends and millennial variations in Holocene temperatures. *Nature*, *554*(7690), 92–96. <https://doi.org/10.1038/nature25464>
- Mathien-Blard, E., & Bassinot, F. (2009). Salinity bias on the foraminifera Mg/Ca thermometry: Correction procedure and implications for past ocean hydrographic reconstructions. *Geochemistry, Geophysics, Geosystems*, *10*, Q12011. <https://doi.org/10.1029/2008GC002353>
- McCulloch, M., Mortimer, G., Esat, T., Xianhua, L., Pillans, B., & Chappell, J. (1996). High resolution windows into early Holocene climate: Sr/Ca coral records from the Huon Peninsula. *Earth and Planetary Science Letters*, *138*(1–4), 169–178. [https://doi.org/10.1016/0012-821x\(95\)00230-a](https://doi.org/10.1016/0012-821x(95)00230-a)
- McGregor, H. V., Fischer, M. J., Gagan, M. K., Fink, D., Phipps, S. J., Wong, H., & Woodroffe, C. D. (2013). A weak El Niño/Southern Oscillation with delayed seasonal growth around 4,300 years ago. *Nature Geoscience*, *6*(11), 949–953. <https://doi.org/10.1038/ngeo1936>
- McGregor, H. V., & Gagan, M. K. (2004). Western Pacific coral $\delta^{18}\text{O}$ records of anomalous Holocene variability in the El Niño–Southern Oscillation. *Geophysical Research Letters*, *31*, L11204. <https://doi.org/10.1029/2004gl019972>
- McGregor, H. V., Gagan, M. K., McCulloch, M. T., Hodge, E., & Mortimer, G. (2008). Mid-Holocene variability in the marine ^{14}C reservoir age for northern coastal Papua New Guinea. *Quaternary Geochronology*, *3*(3), 213–225. <https://doi.org/10.1016/j.quageo.2007.11.002>
- McPhaden, M. J., & Picaut, J. (1990). El Niño–Southern Oscillation displacements of the western equatorial Pacific warm pool. *Science*, *250*(4986), 1385–1388. <https://doi.org/10.1126/science.250.4986.1385>
- Mohtadi, M., Oppo, D. W., Lückge, A., DePol-Holz, R., Steinke, S., Groeneveld, J., et al. (2011). Reconstructing the thermal structure of the upper ocean: Insights from planktic foraminifera shell chemistry and alkenones in modern sediments of the tropical eastern Indian Ocean. *Paleoceanography*, *26*, PA3219. <https://doi.org/10.1029/2011PA002132>
- Mohtadi, M., Oppo, D. W., Steinke, S., Stuet, J.-B. W., De Pol-Holz, R., Hebbeln, D., & Lückge, A. (2011). Glacial to Holocene swings of the Australian-Indonesian monsoon. *Nature Geoscience*, *4*(8), 540–544. <https://doi.org/10.1038/ngeo1209>
- Mohtadi, M., Prange, M., Oppo, D. W., De Pol-Holz, R., Merkel, U., Zhang, X., et al. (2014). North Atlantic forcing of tropical Indian Ocean climate. *Nature*, *509*(7498), 76–80. <https://doi.org/10.1038/nature13196>
- Mohtadi, M., Steinke, S., Lückge, A., Groeneveld, J., & Hathorne, E. C. (2010). Glacial to Holocene surface hydrography of the tropical eastern Indian Ocean. *Earth and Planetary Science Letters*, *292*(1–2), 89–97. <https://doi.org/10.1016/j.epsl.2010.01.024>
- Moy, C. M., Seltzer, G. O., Rodbell, D. T., & Anderson, D. M. (2002). Variability of El Niño/Southern oscillation activity at millennial timescales during the Holocene epoch. *Nature*, *420*(6912), 162–165. <https://doi.org/10.1038/nature01194>
- Neale, R., & Slingo, J. (2003). The maritime continent and its role in the global climate: A GCM study. *Journal of Climate*, *16*(5), 834–848. [https://doi.org/10.1175/1520-0442\(2003\)016<0834:TMCAIR>2.0.CO;2](https://doi.org/10.1175/1520-0442(2003)016<0834:TMCAIR>2.0.CO;2)
- Nürnberg, D., Bijma, J., & Hemleben, C. (1996). Assessing the reliability of magnesium in foraminiferal calcite as a proxy for water mass temperature. *Geochimica et Cosmochimica Acta*, *60*(5), 803–814. [https://doi.org/10.1016/0016-7037\(95\)00446-7](https://doi.org/10.1016/0016-7037(95)00446-7)
- Oppo, D. W., & Rosenthal, Y. (2010). The great Indo-Pacific communicator. *Science*, *328*(5985), 1492–1494. <https://doi.org/10.1126/science.1187273>
- Palmer, T. N., & Mansfield, D. A. (1984). Response of two atmospheric general circulation models to sea-surface temperature anomalies in the tropical East and West Pacific. *Nature*, *310*(5977), 483–485. <https://doi.org/10.1038/310483a0>

- Parnell, A. C., Haslett, J., Allen, J. R. M., Buck, C. E., & Huntley, B. (2008). A flexible approach to assessing synchronicity of past events using Bayesian reconstructions of sedimentation history. *Quaternary Science Reviews*, 27(19–20), 1872–1885. <https://doi.org/10.1016/j.quascirev.2008.07.009>
- Partin, J. W., Cobb, K. M., Adkins, J. F., Clark, B., & Fernandez, D. P. (2007). Millennial-scale trends in West Pacific Warm Pool hydrology since the Last Glacial Maximum. *Nature*, 449(7161), 452–455. <https://doi.org/10.1038/nature06164>
- Partin, J. W., Quinn, T. M., Shen, C.-C., Okumura, Y., Cardenas, M. B., Siringan, F. P., et al. (2015). Gradual onset and recovery of the Younger Dryas abrupt climate event in the tropics. *Nature Communications*, 6(1), 8061. <https://doi.org/10.1038/ncomms9061>
- Pelejero, C., Grimalt, J. O., Heilig, S., Kienast, M., & Wang, L. (1999). High-resolution UK37 temperature reconstructions in the South China Sea over the past 220 kyr. *Paleoceanography*, 14(2), 224–231. <https://doi.org/10.1029/1998PA900015>
- Pena, L. D., Cacho, I., Ferretti, P., & Hall, M. A. (2008). El Niño–Southern Oscillation-like variability during glacial terminations and interlatitudinal teleconnections. *Paleoceanography*, 23, PA3101. <https://doi.org/10.1029/2008pa001620>
- Picaut, J., Ioualalen, M., Menkes, C., Delcroix, T., & McPhaden, M. J. (1996). Mechanism of the zonal displacements of the Pacific warm pool: Implications for ENSO. *Science*, 274(5292), 1486–1489. <https://doi.org/10.1126/science.274.5292.1486>
- Qu, T., Du, Y., & Sasaki, H. (2006). South China Sea throughflow: A heat and freshwater conveyor. *Geophysical Research Letters*, 33, L23617. <https://doi.org/10.1029/2006GL028350>
- Qu, T., & Meyers, G. (2005). Seasonal characteristics of circulation in the southeastern tropical Indian Ocean. *Journal of Physical Oceanography*, 35(2), 255–267. <https://doi.org/10.1175/jpo-2682.1>
- Quadfasel, D., & Cresswell, G. R. (1992). A note on the seasonal variability of the South Java Current. *Journal of Geophysical Research*, 97(C3), 3685–3688. <https://doi.org/10.1029/91jc03056>
- Reimer, P. J., Bard, E., Bayliss, A., Beck, J. W., Blackwell, P. G., Ramsey, C. B., et al. (2013). IntCal13 and Marine13 radiocarbon age calibration curves 0–50,000 years cal BP. *Radiocarbon*, 55(4), 1869–1887. https://doi.org/10.2458/azu_js_rc.55.16947
- Richards, K. J., Kashino, Y., Natarov, A., & Firing, E. (2012). Mixing in the western equatorial Pacific and its modulation by ENSO. *Geophysical Research Letters*, 39, L02604. <https://doi.org/10.1029/2011GL050439>
- Rodgers, K. B., Lohmann, G., Lorenz, S., Schneider, R., & Henderson, G. M. (2003). A tropical mechanism for Northern Hemisphere deglaciation. *Geochemistry, Geophysics, Geosystems*, 4(5), 1046. <https://doi.org/10.1029/2003gc000508>
- Rosell-Melé, A., & Prahl, F. G. (2013). Seasonality of UK'37 temperature estimates as inferred from sediment trap data. *Quaternary Science Reviews*, 72, 128–136. <https://doi.org/10.1016/j.quascirev.2013.04.017>
- Rosenthal, Y., Boyle, E. A., & Slowey, N. (1997). Temperature control on the incorporation of magnesium, strontium, fluorine, and cadmium into benthic foraminiferal shells from Little Bahama Bank: Prospects for thermocline paleoceanography. *Geochimica et Cosmochimica Acta*, 61(17), 3633–3643. [https://doi.org/10.1016/s0016-7037\(97\)00181-6](https://doi.org/10.1016/s0016-7037(97)00181-6)
- Rosenthal, Y., Field, M. P., & Sherrell, R. M. (1999). Precise determination of element/calcium ratios in calcareous samples using sector field inductively coupled plasma mass spectrometry. *Analytical Chemistry*, 71(15), 3248–3253. <https://doi.org/10.1021/ac981410x>
- Rosenthal, Y., Kalansky, J., Morley, A., & Linsley, B. (2017). A paleo-perspective on ocean heat content: Lessons from the Holocene and Common Era. *Quaternary Science Reviews*, 155, 1–12. <https://doi.org/10.1016/j.quascirev.2016.10.017>
- Rosenthal, Y., Linsley, B. K., & Oppo, D. W. (2013). Pacific Ocean heat content during the past 10,000 years. *Science*, 342(6158), 617–621. <https://doi.org/10.1126/science.1240837>
- Rosenthal, Y., Oppo, D. W., & Linsley, B. K. (2003). The amplitude and phasing of climate change during the last deglaciation in the Sulu Sea, western equatorial Pacific. *Geophysical Research Letters*, 30(8), 1428. <https://doi.org/10.1029/2002GL016612>
- Rosenthal, Y., Perron-Cashman, S., Lear, C. H., Bard, E., Barker, S., Billups, K., et al. (2004). Laboratory inter-comparison study of Mg/Ca and Sr/Ca measurements in planktonic foraminifera for paleoceanographic research. *Geophysics Geochemistry Geosystems*, 5(4). <https://doi.org/10.1029/2003GC000650>
- Sachs, J. P., Pahnke, K., Smittenberg, R., & Zhang, Z. (2007). Biomarker indicators of past climate. In S. Elias & C. Mock (Eds.), *Encyclopedia of Quaternary Science* (2nd ed., pp. 775–779). Amsterdam: Elsevier Science.
- Sadekov, A. Y., Ganeshram, R., Pichevin, L., Berdin, R., McClymont, E., Elderfield, H., & Tudhope, A. W. (2013). Palaeoclimate reconstructions reveal a strong link between El Niño–Southern Oscillation and Tropical Pacific mean state. *Nature Communications*, 4, 2692. <https://doi.org/10.1038/ncomms3692>
- Schlitzer, R. (2015). Data analysis and visualization with Ocean Data View. *CMOS Bulletin SCMO*, 43(1), 9–13.
- Schneider, T., Bischoff, T., & Haug, G. H. (2014). Migrations and dynamics of the Intertropical Convergence Zone. *Nature*, 513(7516), 45–53. <https://doi.org/10.1038/nature13636>
- Schott, F. A., & McCreary, J. P. (2001). The monsoon circulation of the Indian Ocean. *Progress in Oceanography*, 51(1), 1–123. [https://doi.org/10.1016/S0079-6611\(01\)00083-0](https://doi.org/10.1016/S0079-6611(01)00083-0)
- Schröder, J. F., Holbourn, A., Kuhnt, W., & Küssner, K. (2016). Variations in sea surface hydrology in the southern Makassar Strait over the past 26 kyr. *Quaternary Science Reviews*, 154, 143–156. <https://doi.org/10.1016/j.quascirev.2016.10.018>
- Schröder, J. F., Kuhnt, W., Holbourn, A., Beil, S., Zhang, P., Hendrizan, M., & Xu, J. (2018). Deglacial warming and hydroclimate variability in the central Indonesian Archipelago. *Paleoceanography and Paleoclimatology*, 33, 974–993. <https://doi.org/10.1029/2018pa003323>
- Setiawan, R. Y., Mohtadi, M., Southon, J., Groeneveld, J., Steinke, S., & Hebbeln, D. (2015). The consequences of opening the Sunda Strait on the hydrography of the eastern tropical Indian Ocean. *Paleoceanography*, 30, 1358–1372. <https://doi.org/10.1002/2015pa002802>
- Sprintall, J., Gordon, A. L., Koch-Larrouy, A., Lee, T., Potemra, J. T., Pujiana, K., & Wijffels, S. E. (2014). The Indonesian seas and their role in the coupled ocean–climate system. *Nature Geoscience*, 7(7), 487–492. <https://doi.org/10.1038/ngeo2188>
- Sprintall, J., Wijffels, S. E., Molcard, R., & Jaya, I. (2009). Direct estimates of the Indonesian Throughflow entering the Indian Ocean: 2004–2006. *Journal of Geophysical Research*, 114, C07001. <https://doi.org/10.1029/2008JC005257>
- Steinke, S., Glatz, C., Mohtadi, M., Groeneveld, J., Li, Q., & Jian, Z. (2011). Past dynamics of the East Asian monsoon: No inverse behaviour between the summer and winter monsoon during the Holocene. *Global and Planetary Change*, 78(3–4), 170–177. <https://doi.org/10.1016/j.gloplacha.2011.06.006>
- Steinke, S., Kienast, M., Groeneveld, J., Lin, L.-C., Chen, M.-T., & Rendle-Bühning, R. (2008). Proxy dependence of the temporal pattern of deglacial warming in the tropical South China Sea: toward resolving seasonality. *Quaternary Science Reviews*, 27(7–8), 688–700. <https://doi.org/10.1016/j.quascirev.2007.12.003>
- Steinke, S., Kienast, M., Pflaumann, U., Weinelt, M., & Stattegger, K. (2001a). A high-resolution sea-surface temperature record from tropical South China Sea (16,500–3,000 yr B.P.). *Quaternary Research*, 55(3), 352–362. <https://doi.org/10.1006/qres.2001.2235>
- Steinke, S., Kienast, M., Pflaumann, U., Weinelt, M., & Stattegger, K. (2001b). A high-resolution sea-surface temperature record from the tropical South China Sea (16,500–3,000 yr B.P.). *Quaternary Research*, 55(3), 352–362. <https://doi.org/10.1006/qres.2001.2235>

- Stott, L., Cannariato, K., Thunell, R., Haug, G. H., Koutavas, A., & Lund, S. (2004). Decline of surface temperature and salinity in the western tropical Pacific Ocean in the Holocene epoch. *Nature*, *431*(7004), 56–59. <https://doi.org/10.1038/nature02903>
- Sun, Y., Oppo, D. W., Xiang, R., Liu, W., & Gao, S. (2005). Last deglaciation in the Okinawa Trough: Subtropical northwest Pacific link to Northern Hemisphere and tropical climate. *Paleoceanography*, *20*, PA4005. <https://doi.org/10.1029/2004pa001061>
- Takahashi, T., Sutherland, S. C., and Kozyr, A. V. (2017). Global ocean surface water partial pressure of CO₂ database: Measurements performed during 1957–2016 (version 2016), 3.
- Tian, Z., Li, T., & Jiang, D. (2018). Strengthening and westward shift of the tropical Pacific Walker circulation during the mid-Holocene: PMIP simulation results. *Journal of Climate*, *31*(6), 2283–2298. <https://doi.org/10.1175/JCLI-D-16-0744.1>
- Tierney, J. E., Oppo, D. W., LeGrande, A. N., Huang, Y., Rosenthal, Y., & Linsley, B. K. (2012). The influence of Indian Ocean atmospheric circulation on Warm Pool hydroclimate during the Holocene epoch. *Journal of Geophysical Research*, *117*, D19108. <https://doi.org/10.1029/2012JD018060>
- Timmermann, A., Lorenz, S. J., An, S.-I., Clement, A., & Xie, S.-P. (2007). The effect of orbital forcing on the mean climate and variability of the tropical Pacific. *Journal of Climate*, *20*(16), 4147–4159. <https://doi.org/10.1175/jcli4240.1>
- Timmermann, A., Sachs, J., & Timm, O. E. (2014). Assessing divergent SST behavior during the last 21 ka derived from alkenones and *G. ruber*-Mg/Ca in the equatorial Pacific. *Paleoceanography*, *29*, 680–696. <https://doi.org/10.1002/2013PA002598>
- Toggweiler, J. R., & Lea, D. W. (2010). Temperature differences between the hemispheres and ice age climate variability. *Paleoceanography*, *25*, PA2212. <https://doi.org/10.1029/2009pa001758>
- Trenberth, K. E., Branstator, G. W., Karoly, D., Kumar, A., Lau, N.-C., & Ropelewski, C. (1998). Progress during TOGA in understanding and modeling global teleconnections associated with tropical sea surface temperatures. *Journal of Geophysical Research*, *103*(C7), 14,291–14,324. <https://doi.org/10.1029/97JC01444>
- Tudhope, A. W., Chilcott, C. P., McCulloch, M. T., Cook, E. R., Chappell, J., Ellam, R. M., et al. (2001). Variability in the El Niño–Southern Oscillation through a glacial-interglacial cycle. *Science*, *291*(5508), 1511–1517. <https://doi.org/10.1126/science.1057969>
- Ueki, I., Kashino, Y., & Kuroda, Y. (2003). Observation of current variations off the New Guinea coast including the 1997–1998 El Niño period and their relationship with Sverdrup transport. *Journal of Geophysical Research*, *108*(C7), 3243. <https://doi.org/10.1029/2002jc001611>
- van Sebille, E., Sprintall, J., Schwarzkopf, F. U., Sen Gupta, A., Santoso, A., England, M. H., et al. (2014). Pacific-to-Indian Ocean connectivity: Tasman leakage, Indonesian Throughflow, and the role of ENSO. *Journal of Geophysical Research: Oceans*, *119*, 1365–1382. <https://doi.org/10.1002/2013jc009525>
- Visser, K., Thunell, R., & Stott, L. (2003). Magnitude and timing of temperature change in the Indo-Pacific warm pool during deglaciation. *Nature*, *421*(6919), 152–155. <https://doi.org/10.1038/nature01297>
- Wang, H., & Mehta, V. M. (2008). Decadal variability of the Indo-Pacific warm pool and its association with atmospheric and oceanic variability in the NCEP–NCAR and SODA reanalyses. *Journal of Climate*, *21*(21), 5545–5565. <https://doi.org/10.1175/2008jcli2049.1>
- Wang, P., Li, Q., & Li, C.-F. (2014). Chapter 2—General outline of the China Seas. In Q. L. Pinxian Wang & L. Chun-Feng (Eds.), *Developments in Marine Geology* (pp. 11–72). Amsterdam: Elsevier.
- Wang, Y., Cheng, H., Edwards, R. L., He, Y., Kong, X., An, Z., et al. (2005). The Holocene Asian monsoon: Links to solar changes and North Atlantic climate. *Science*, *308*(5723), 854–857. <https://doi.org/10.1126/science.1106296>
- Wang, Y., Cheng, H., Edwards, R. L., Kong, X., Shao, X., Chen, S., et al. (2008). Millennial- and orbital-scale changes in the East Asian monsoon over the past 224,000 years. *Nature*, *451*(7182), 1090–1093. <https://doi.org/10.1038/nature06692>
- Weller, E., Min, S.-K., Cai, W., Zwiers, F. W., Kim, Y.-H., & Lee, D. (2016). Human-caused Indo-Pacific warm pool expansion. *Science Advances*, *2*(7), e1501719. <https://doi.org/10.1126/sciadv.1501719>
- White, S. M., Ravelo, A. C., & Polissar, P. J. (2018). Dampened El Niño in the early and mid-Holocene due to insolation-forced warming/deepening of the thermocline. *Geophysical Research Letters*, *45*(1), 316–326. <https://doi.org/10.1002/2017gl075433>
- Wyrski, K. (1987). Indonesian Throughflow and associated pressure gradient. *Journal of Geophysical Research*, *92*(C12), 12,941–12,946. <https://doi.org/10.1029/JC092iC12p12941>
- Wyrski, K. (1989). Some thoughts about the west Pacific warm pool, paper presented at Proceedings of the Western Pacific International Meeting and Workshop on TOGA COARE.
- Xu, J., Holbourn, A., Kuhnt, W., Jian, Z., & Kawamura, H. (2008). Changes in the thermocline structure of the Indonesian outflow during Terminations I and II. *Earth and Planetary Science Letters*, *273*(1–2), 152–162. <https://doi.org/10.1016/j.epsl.2008.06.029>
- Yan, X.-H., Ho, C.-R., Zheng, Q., & Klemas, V. (1992). Temperature and size variabilities of the Western Pacific Warm Pool. *Science*, *258*(5088), 1643–1645. <https://doi.org/10.1126/science.258.5088.1643>
- Zhang, P., Zuraida, R., Rosenthal, Y., Holbourn, A., Kuhnt, W., & Xu, J. (2018). Geochemical characteristics from tests of four modern planktonic foraminiferal species in the Indonesian Throughflow region and their implications. *Geoscience Frontiers*, *10*(2), 505–516. <https://doi.org/10.1016/j.gsf.2018.01.011>
- Zhao, M., Huang, C.-Y., Wang, C.-C., & Wei, G. (2006). A millennial-scale U37K' sea-surface temperature record from the South China Sea (8°N) over the last 150 kyr: Monsoon and sea-level influence. *Palaeogeography, Palaeoclimatology, Palaeoecology*, *236*(1–2), 39–55. <https://doi.org/10.1016/j.palaeo.2005.11.033>